CMS-TOP-17-013

arXiv:1808.07340v2 [hep-ex] 2 Dec 2018

Measurement of jet substructure observables in $t\bar{t}$ events from proton-proton collisions at $\sqrt{s} = 13\,\text{TeV}$

The CMS Collaboration*

Abstract

A measurement of jet substructure observables is presented using $t\bar{t}$ events in the lepton+jets channel from proton-proton collisions at $\sqrt{s} = 13\,\text{TeV}$ recorded by the CMS experiment at the LHC, corresponding to an integrated luminosity of $35.9\,\text{fb}^{-1}$. Multiple jet substructure observables are measured for jets identified as bottom, light-quark, and gluon jets, as well as for inclusive jets (no flavor information). The results are unfolded to the particle level and compared to next-to-leading-order predictions from POWHEG interfaced with the parton shower generators PYTHIA 8 and HERWIG 7, as well as from SHERPA 2 and DIRE 2. A value of the strong coupling at the Z boson mass, $\alpha_S(m_Z) = 0.115^{+0.015}_{-0.013}$, is extracted from the substructure data at leading-order plus leading-log accuracy.

*See Appendix A for the list of collaboration members

1 Introduction

The confinement property of quantum chromodynamics (QCD) renders isolated quarks and gluons unobservable. Instead, strongly interacting partons produced in high-energy hadron-hadron collisions initiate a cascade of lower-energy quarks and gluons that eventually hadronize into a jet composed of colorless hadrons. Monte Carlo (MC) event generators [1] describe reasonably well both the perturbative cascade, dominated by soft gluon emissions and collinear parton splittings, as well as the final hadronization (via nonperturbative string or cluster models at the end of the parton shower below some cutoff scale of the order of $1\,\text{GeV}$). The details of the perturbative radiation phase have been studied at previous colliders (Tevatron [2–4], HERA [5–7]), and the various parameters of the parton fragmentation models have been tuned to match jet data from e^+e^- collisions, collected mostly at LEP [8–13] and SLC [14, 15].

Precise measurements of jet properties at the LHC allow improvements in the experimental techniques and theoretical predictions for heavy-quark/light-quark/gluon discrimination, as well as in the identification of merged jets from Lorentz-boosted heavy particle decays [16, 17]. They also give information about the limits and applicability of the current parton shower and fragmentation models in the gluon-dominated environment of proton-proton (pp) collisions, rather than the quark-dominated one, as in the e^+e^- case [18]. In addition, jet substructure studies test QCD in the infrared- and/or collinear-safe limits where recent calculations [19] provide analytical predictions with increasingly accurate higher-order corrections, including, e.g., up to next-to-leading-order (NLO) terms [20], and beyond next-to-leading-logarithmic (NLL) resummations [21] for some observables.

Jet shapes and substructure have been measured in pp collisions at $\sqrt{s} = 7\,\text{TeV}$ by the ATLAS Collaboration in dijet events [22, 23], and by the CMS Collaboration in dijet and W/Z+jet events [24]. Furthermore, jet substructure was measured in dijet events at $8\,\text{TeV}$ by CMS [25] and at $13\,\text{TeV}$ by ATLAS [26] and CMS [27]. Measurements of jet shapes have also been carried out by ATLAS using events containing top quark-antiquark ($t\bar{t}$) pairs at $7\,\text{TeV}$ [28], exploiting for the first time the possibility of comparing the properties of bottom and light-quark jets from the top quark decays. The mass distribution of boosted top quark candidates was measured by CMS at $8\,\text{TeV}$ [29].

The analysis presented here uses jet samples obtained from fully resolved $t\bar{t}$ lepton+jets events, where one of the W bosons decays to a charged lepton (electron or muon) and the corresponding neutrino, while the other W boson decays to quarks, yielding two separate jets. Various jet substructure observables are measured in order to characterize the jet evolution, such as generalized angularities, eccentricity, groomed momentum fraction, $\mathcal{N}$-subjettiness ratios, and energy correlation functions. For comparison with theory predictions, the measured distributions are corrected for detector effects, unfolding them to the particle level that is defined using stable particles with decay length larger than $10\,\text{mm}$.

The measurements are performed using data recorded at $\sqrt{s} = 13\,\text{TeV}$ by the CMS detector described in Section 2. Section 3 contains details of the data and simulated samples. Events are reconstructed and selected using the algorithms described in Section 4. The unfolding to the particle-level of the observables of interest and their associated systematic uncertainties are described in Section 5. The jet substructure variables under investigation are defined and the results presented in Section 6. The $t\bar{t}$ lepton+jets topology allows for sorting the jets into samples enriched in bottom quarks, light quarks from the W boson decays, or gluons stemming from initial-state radiation (ISR), as discussed in Section 7. The correlation between jet substructure observables, and their level of agreement to different MC predictions are studied in Section 8. Finally, an extraction of the strong coupling from jet substructure observables is

presented in Section 9.

2 The CMS detector

The central feature of the CMS apparatus is a superconducting solenoid of 6 m internal diameter, providing a magnetic field of 3.8 T. Within the solenoid volume are a silicon pixel and strip tracker, a lead tungstate crystal electromagnetic calorimeter (ECAL), and a brass and scintillator hadron calorimeter (HCAL), each composed of a barrel and two endcap sections. Forward calorimeters extend the pseudorapidity (η) coverage provided by the barrel and endcap detectors. Muons are detected in gas-ionization chambers embedded in the steel flux-return yoke outside the solenoid. Events of interest are selected using a two-tiered trigger system [30]. The first level (L1), composed of custom hardware processors, uses information from the calorimeters and muon detectors to select events at a rate of around 100 kHz within a time interval of less than 4 μs. The second level, known as the high-level trigger (HLT), consists of a farm of processors running a version of the full event reconstruction software optimized for fast processing, and reduces the event rate to around 1 kHz before data storage.

A more detailed description of the CMS detector, together with a definition of the coordinate system used and the relevant kinematic variables, can be found in Ref. [31].

3 Data and simulated samples

The measurements presented in this paper are based on pp collision data recorded by the CMS experiment during the 2016 run at $\sqrt{s} = 13$ TeV, corresponding to an integrated luminosity of 35.9 fb^{-1}. The average number of pp interactions per bunch crossing is $\langle \mu \rangle = 27$.

The $t\bar{t}$ signal process is simulated with the POWHEG v2 [32–35] matrix-element (ME) generator at NLO accuracy with a top quark mass value $m_t = 172.5$ GeV. The $t\bar{t}$ samples are normalized to the cross section calculated at next-to-next-to-leading order [36]. The $t\bar{t}$+W, $t\bar{t}$+Z, WZ, W+jets, and ZZ→2ℓ2q (where ℓ denotes a lepton) background processes are generated at NLO using MADGRAPH5_aMC@NLO v2.2.2 [37] with the FxFx merging scheme [38] for the jets from the ME generator and the parton shower. The Drell–Yan background is computed at leading order (LO) with the MLM merging prescription [39]. The WW, ZZ→2ℓ2ν, and tW backgrounds are generated with POWHEG v2 [40, 41], while single top quark t-channel production is simulated using POWHEG v2 [42] complemented with MADSPIN [43, 44]. QCD multijet background events are generated with PYTHIA v8.219 [45]. The NNPDF3.0 NLO [46] set of parton distribution functions (PDFs), and the strong coupling $\alpha_S(m_Z) = 0.118$ are used in the ME calculations.

The ME generators are interfaced with PYTHIA 8 for parton shower, hadronization, and underlying multiparton interactions (MPI). PYTHIA 8 implements a dipole shower ordered in transverse momentum (p_T), with ME corrections [47] for the leading emissions in the top quark and W boson decays. The hadronization of quarks and gluons into final hadrons is described by the Lund string model [48, 49], with the Bowler–Lund fragmentation function for heavy quarks [50]. The CUETP8M2 tune, taking into account $t\bar{t}$ jet multiplicity data [51], is used for the $t\bar{t}$ signal and the single top quark background, while the CUETP8M1 tune [52] is used for the remaining processes. Additional $t\bar{t}$ samples were generated with parameter variations to estimate systematic uncertainties (Section 5), as well as with POWHEG interfaced with HERWIG++ v2.7.1 [53]. In HERWIG++, the parton shower follows angular-ordered radiation [54], and the hadronization is described by the cluster model [55].

The generated events are processed with the CMS detector simulation based on GEANT4 [56].

Table 1: Overview of the theoretical accuracy and $\alpha_S^{\mathrm{FSR}}(m_Z)$ settings of the generator setups used for predicting the jet substructure. The acronym "nLL" stands for approximate next-to-leading-log accuracy.

	POWHEG + PYTHIA 8			POWHEG +	SHERPA 2	DIRE 2
	FSR-down	Nominal	FSR-up	HERWIG 7		
$\mathrm{t\bar{t}}$ production	NLO	NLO	NLO	NLO	NLO	LO
t/W decay	NLO	NLO	NLO	NLO	LO	LO
Decay emission	LO	LO	LO	LO	LL	nLL
Shower accuracy	LL	LL	LL	LL	LL	nLL
$\alpha_S^{\mathrm{FSR}}(m_Z)$	0.1224	0.1365	0.1543	0.1262	0.118	0.1201
Evolution	One-loop	One-loop	One-loop	Two-loop	Two-loop	Two-loop
Scheme	$\overline{\mathrm{MS}}$	$\overline{\mathrm{MS}}$	$\overline{\mathrm{MS}}$	$\overline{\mathrm{MS}}$	CMW	$\overline{\mathrm{MS}}$

Additional pp interactions in the same bunch crossing (pileup) are taken into account by adding detector hits of simulated minimum-bias events before event reconstruction. The simulation is weighted to reproduce the pileup conditions observed in the data. The simulated events are also corrected for the difference in performance between data and simulation of the trigger paths as well as in lepton identification and isolation efficiencies with scale factors depending on p_T and η. The simulated tracking efficiency is corrected with scale factors that depend on the track η.

Additional predictions are generated without detector simulation for comparisons at the particle level. POWHEG v2 is interfaced with HERWIG v7.1.1 [57] using the angular-ordered shower. In addition, a prediction from SHERPA v2.2.4 [58] with MC@NLO [59] corrections is included. The parton shower in SHERPA 2 is based on the Catani–Seymour dipole factorization [60], and hadrons are formed by a modified cluster hadronization model [61]. The parton shower predictions from PYTHIA 8, HERWIG 7 and SHERPA 2 have leading-log (LL) accuracy, with the option to use Catani–Marchesini–Webber (CMW) rescaling of α_S to account for next-to-leading corrections to soft gluon emissions [62]. Events are also generated with DIRE v2.002 [63], a dipole-like parton shower ordered in (soft) p_T available as a plugin for PYTHIA 8. DIRE 2 includes two- and three-loop cusp effects for soft emissions and partial NLO collinear evolution [64, 65], denoted nLL accuracy hereafter. The values of the QCD coupling in the final-state radiation (FSR) showers, $\alpha_S^{\mathrm{FSR}}(m_Z)$, are summarized in Table 1. They are obtained from tuning the generator to LEP data using its default settings, with the exception of SHERPA 2, where the $\alpha_S(m_Z)$ is chosen to be consistent between ME calculation and parton shower. The PYTHIA 8 and SHERPA 2 generators apply a model where the MPIs are interleaved with parton showering [66], while HERWIG 7 models the overlap between the colliding protons through a Fourier transform of the electromagnetic form factor, which plays the role of an effective inverse proton radius [67–70]. Depending on the amount of proton overlap, the contribution of generated MPIs varies in the simulation. The MPI parameters of all generators are tuned to measurements in pp collisions at the LHC [52].

4 Event reconstruction and selection

The particle-flow (PF) event algorithm [71] aims to reconstruct and identify each individual particle in an event with an optimized combination of information from the various elements of the CMS detector. The energy of photons is directly obtained from the ECAL measurement, corrected for zero-suppression effects. The energy of electrons is determined from a combina-

tion of the electron momentum at the primary interaction vertex as determined by the tracker, the energy of the corresponding ECAL cluster, and the energy sum of all bremsstrahlung photons spatially compatible with originating from the electron track. The energy of muons is obtained from the curvature of the corresponding track. The energy of charged hadrons is determined from a combination of their momentum measured in the tracker and the matching ECAL and HCAL energy deposits, corrected for zero-suppression effects and for the response function of the calorimeters to hadronic showers. Finally, the energy of neutral hadrons is obtained from the corresponding corrected ECAL and HCAL energies.

For each event, hadronic jets are clustered from these reconstructed particles using the infrared- and collinear-safe anti-k_T algorithm [72] with a distance parameter $R = 0.4$, as implemented in FASTJET 3.1 [73]. The jet momentum is determined as the vectorial sum of all particle momenta in this jet, and is found in the simulation to agree with the true jet momentum within 5 to 10% over the whole p_T spectrum and detector acceptance. Jet energy corrections are derived from the simulation, and are confirmed with in situ measurements of the energy balance in dijet, multijet, photon+jet, and leptonically-decaying Z+jet events. The jet energy resolution amounts typically to 15% at 10 GeV, 8% at 100 GeV, and 4% at 1 TeV [74].

The event selection is based on the $t\bar{t}$ lepton+jets decay topology, where data samples are collected using electron or muon triggers with a p_T threshold of 32 or 24 GeV, respectively. In the offline selection, the relative isolation of electrons (muons) is defined as the scalar sum of PF candidates p_T within a cone of $\Delta R = \sqrt{(\Delta\eta)^2 + (\Delta\phi)^2} = 0.3\,(0.4)$ (where $\Delta\eta$ and $\Delta\phi$ are the separations in pseudorapidity and azimuth (in radians) of lepton and PF candidate) around the lepton direction, divided by the lepton p_T, and is required to be smaller than 0.06 (0.15). Leptons have to fulfill tight identification criteria, taking into account track properties and energy deposits, based on their expected signature in the detector. Exactly one isolated lepton (electron or muon) is required, having $p_T > 34\,(26)$ GeV and $|\eta| < 2.1\,(2.4)$ for electrons (muons) [75, 76]. The event is not selected in the presence of a second loosely-identified lepton with $p_T > 15$ GeV and $|\eta| < 2.4$, in order to suppress Drell–Yan and $t\bar{t}$ dilepton events. Furthermore, the events are required to contain at least four jets with $p_T > 30$ GeV and $|\eta| < 2.5$, of which at least two are required to be b-tagged. The Combined Secondary Vertex (CSVv2) b tagging algorithm is used at a working point, which has a mean efficiency of 63% for the correct identification of a bottom jet and a probability of 0.9% for misidentifying light-flavor (uds or gluon) jets, and 12% for charm jets in a $t\bar{t}$ sample [77, 78]. Finally, at least two untagged jets are required to yield a W boson candidate with an invariant mass satisfying $|m_{jj} - 80.4\,\text{GeV}| < 15$ GeV, and these jets are composing the light-quark-enriched jet sample. Events with no (one) W boson candidate contain no (two) light-quark-enriched jets. Events are allowed to contain more than one W boson candidate, leading to more than two jets associated to the light-quark-enriched sample. The number of events selected in data is 287 239, with $285\,000 \pm 38\,000$ expected. The selected sample is composed of 93.8% $t\bar{t}$ events as estimated from simulation. The multiplicities of bottom-quark jets and untagged jets compatible with W boson candidates at the reconstructed level are presented in Fig. 1 and show good agreement between data and MC prediction.

At the particle level in simulated events, the unfolded jet observables are defined in a phase space region described hereafter. More details about the algorithms and relevant studies can be found in Ref. [79]. Leptons are required to be prompt (i.e., not from hadron decays), and the momenta of prompt photons located within a cone of radius $\Delta R = 0.1$ are added to the lepton momentum to account for FSR, referred to as "dressing". Exactly one lepton with $p_T > 26$ GeV and $|\eta| < 2.4$ is required, while events containing additional dressed leptons fulfilling looser kinematic criteria ($p_T > 15$ GeV, $|\eta| < 2.4$) are rejected. Jets are clustered from stable particles excluding neutrinos and the dressed leptons with the anti-k_T algorithm using a distance pa-
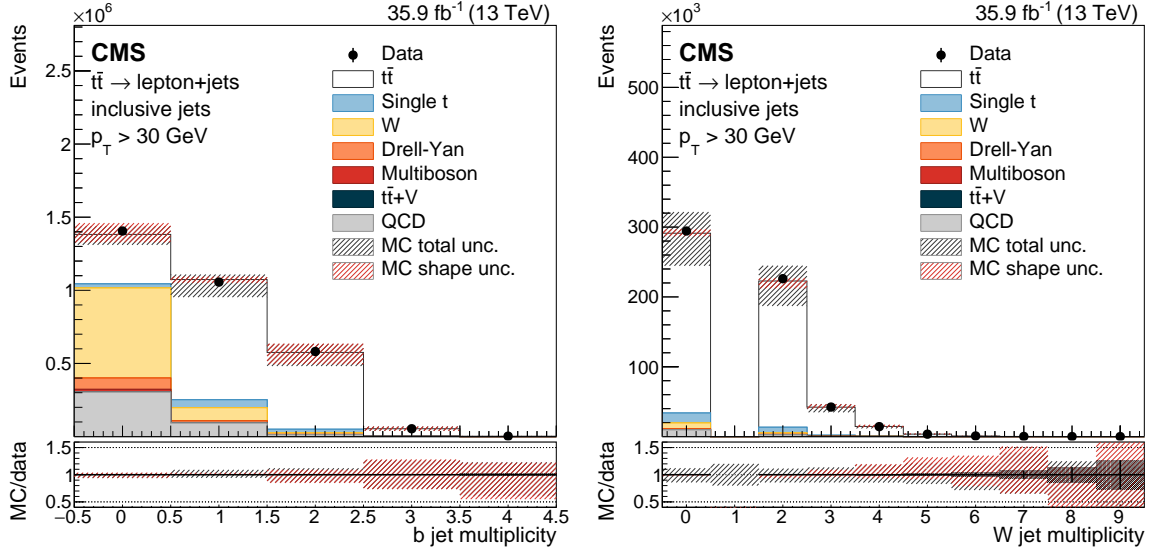
Figure 1: Multiplicity of b-tagged jets in events with exactly one isolated lepton and four jets (left), and multiplicity of untagged jets yielding a W boson candidate with $|m_{jj} - 80.4\,\text{GeV}| < 15\,\text{GeV}$ after requiring two b-tagged jets (right). These reconstruction-level plots show the sum of the expected contributions from each process (stacked histograms) compared to the data points (upper panels), and the ratio of the MC prediction (POWHEG + PYTHIA 8) to the data (lower panels) where the black shaded band represents the statistical uncertainty on the data. The systematic uncertainties on the MC prediction are represented by hatched areas, taking into account either the total uncertainty or shape variations only.

rameter $R = 0.4$. At least four jets with $p_T > 30\,\text{GeV}$ and $|\eta| < 2.5$ are required. In order to identify the jet flavor at particle level, decayed heavy hadrons are included in the jet clustering after scaling their momenta by 10^{-20} (known as "ghost" tagging [80]). A jet is identified as a bottom jet when it contains at least one bottom hadron, and two b-tagged jets are required in the event. At least one pair of untagged jet candidates needs to fulfill the W boson mass constraint $|m_{jj} - 80.4\,\text{GeV}| < 15\,\text{GeV}$. The p_T distributions at the particle level are shown in Fig. 2 for different MC generators and different jet flavor samples (cf. Section 7 for the flavor definitions).

5 Unfolding and systematic uncertainties

All jet substructure distributions described in the following sections are unfolded to the particle level. Unregularized unfolding as implemented in the TUNFOLD package [81] is used to correct the background-subtracted data distributions to the particle level by minimizing $\chi^2 = (y - K\lambda)^T V_{yy}^{-1}(y - K\lambda)$, where K is the particle-to-reconstructed phase space migration matrix, V_{yy} is an estimate of the covariance of the observations y, and λ is the particle level expectation. The binning of the migration matrix takes into account the resolution of the observables. We define purity as the fraction of reconstructed events that are generated in the same bin, and stability as the fraction of generated events that are reconstructed in the same bin, divided by the overall reconstruction efficiency per bin. Both quantities are $\geq 50\%$ in most bins. In each bin the fractional contribution of jets from $t\bar{t}$ events that pass selection criteria at detector- but not at particle-level is subtracted. The unfolded distributions are normalized to unity within the chosen axis range, i.e., the overflow is discarded. Pseudo-experiments are conducted by unfolding pseudo-data distributions sampled from simulated $t\bar{t}$ events and confirm that the unfolding does not introduce any bias and yields a correct estimate of the statistical
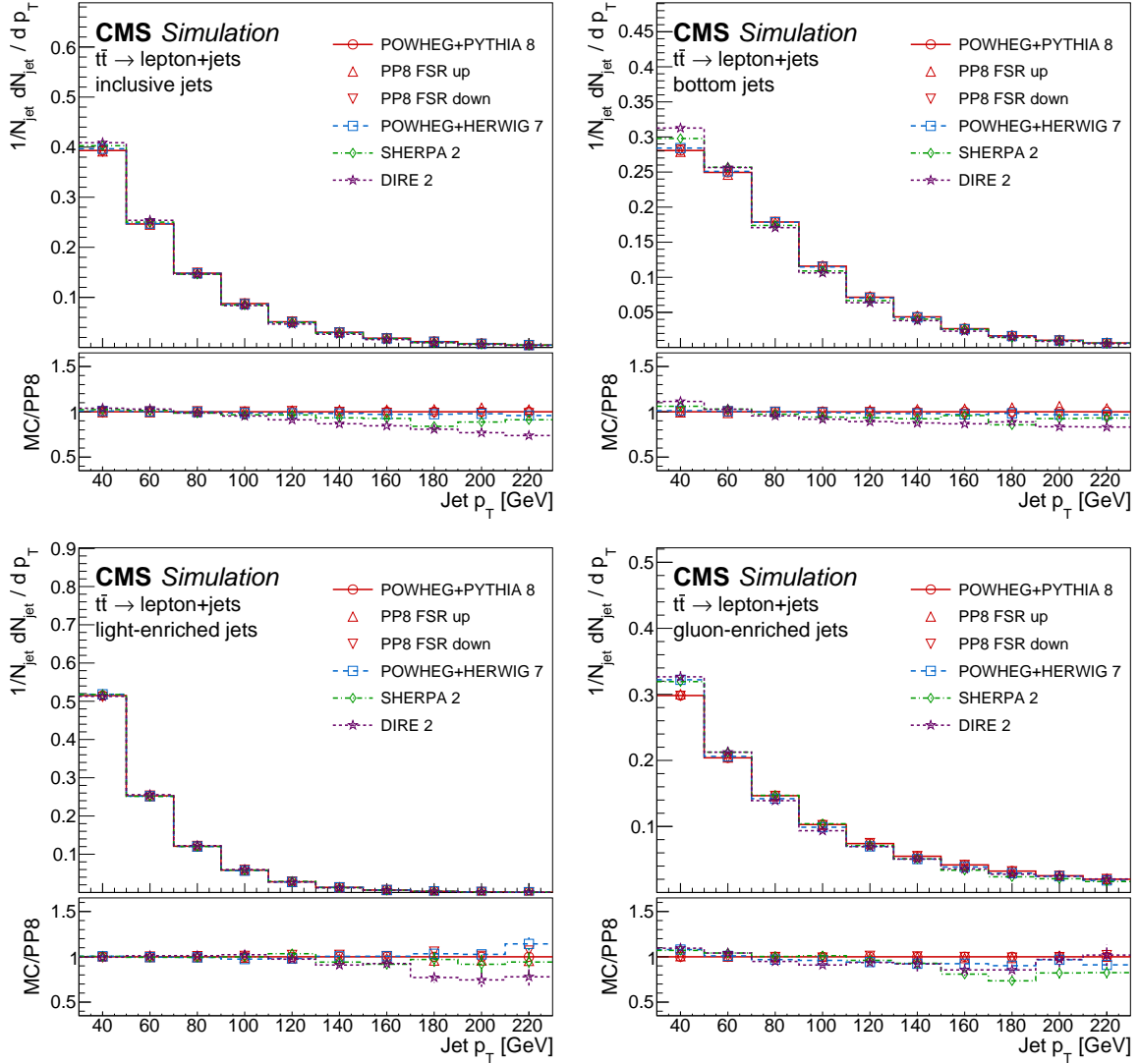
Figure 2: Transverse momentum distribution at the particle level for inclusive jets (upper left), bottom-quark jets (upper right), light-quark-enriched jets (lower left), and gluon-enriched jets (lower right). The sub-panels show the corresponding ratios of the different MC predictions over POWHEG + PYTHIA 8 (PP8).

uncertainties.

While the central result is unfolded using POWHEG + PYTHIA 8 with the nominal data-to-simulation correction factors, systematic uncertainties are assessed by using migration matrices obtained from alternative samples and systematic variations of the correction factors used in this analysis. The uncertainty in the number of pileup events is estimated by changing the total inelastic pp cross section by $\pm 5\%$ [82]. The data-to-simulation scale factors for lepton trigger and selection efficiencies are varied within their uncertainties. The energy scale of jets is varied within its uncertainty, as a function of the jet p_T, η, and flavor, as well as the jet resolution, depending on its η. The b tagging efficiency and misidentification probabilities are varied within their uncertainties. A data-to-simulation tracking efficiency scale factor is determined as a function of η for charged pions. An uncertainty of 3–6% is assigned to the tracking scale factor, assumed to be correlated across run periods and detector regions, resulting in a global up or down variation. The cross sections of the most important backgrounds contributions are scaled within their uncertainties: 5% for single top quark [83–86], 10% for W + 1 jet, and 33% for W + 2 jets [37, 38] processes. We assume an uncertainty of 100% on the QCD multijet background predicted by the MC.

The uncertainties in the modeling of the $t\bar{t}$ lepton+jets signal are estimated using migration matrices derived from fully simulated samples with the following variations. The renormalization and factorization scales in the ME calculation are varied by factors of 0.5 and 2.0 using weights. CT14 (NLO) [87] and MMHT2014 (NLO) [88] are used as alternative PDF sets. The scales for ISR and FSR in the parton shower are varied independently by factors of 0.5 and 2.0 with respect to their default values. The h_{damp} parameter regulating the real emissions in POWHEG is varied from its central value of $1.58\,m_t$ using samples with h_{damp} set to $0.99\,m_t$ and $2.24\,m_t$, as obtained from tuning to $t\bar{t}$ data at $\sqrt{s} = 8\,\text{TeV}$ [51]. Additional samples are generated with the MPI tune varied within its uncertainties. For estimating the uncertainty due to color reconnection (CR), we consider the difference between including and excluding (default) the top quark decay products in the default model which fuses the color flow of different systems to minimize the total color string length [66]. Two additional models are taken into account, including the top quark decay products: a new model respecting QCD color rules [89], and the gluon move scheme [90] for minimizing the total string length. An additional sample is generated using POWHEG interfaced with HERWIG++ for testing an alternative model of parton shower, hadronization, MPI, and CR. The b fragmentation function is varied to cover e^+e^- data at the Z pole [10, 15, 91, 92] with the Bowler–Lund [50] and the Peterson [93] parametrizations. Semileptonic branching fractions of b hadrons are varied within their measured values [94]. The top quark mass is measured by CMS with an uncertainty of $\pm 0.49\,\text{GeV}$ [95] and samples in this analysis are generated with $\pm 1\,\text{GeV}$ in order to estimate its impact on the jet substructure measurements. The p_T distribution of the top quark was found to be in disagreement with NLO predictions by recent CMS measurements at $\sqrt{s} = 13\,\text{TeV}$ [96, 97]. Therefore, the full data-to-simulation difference in the top quark p_T distribution is taken as an uncertainty. The effects of the most important systematic uncertainties on selected observables (cf. Sections 6 and 8) are shown in Fig. 3. The uncertainties from the FSR modeling are shown to be significantly smaller than the respective full effect of the variations at the particle level, demonstrating the stability of the unfolded measurement against the MC model used for constructing the migration matrices.
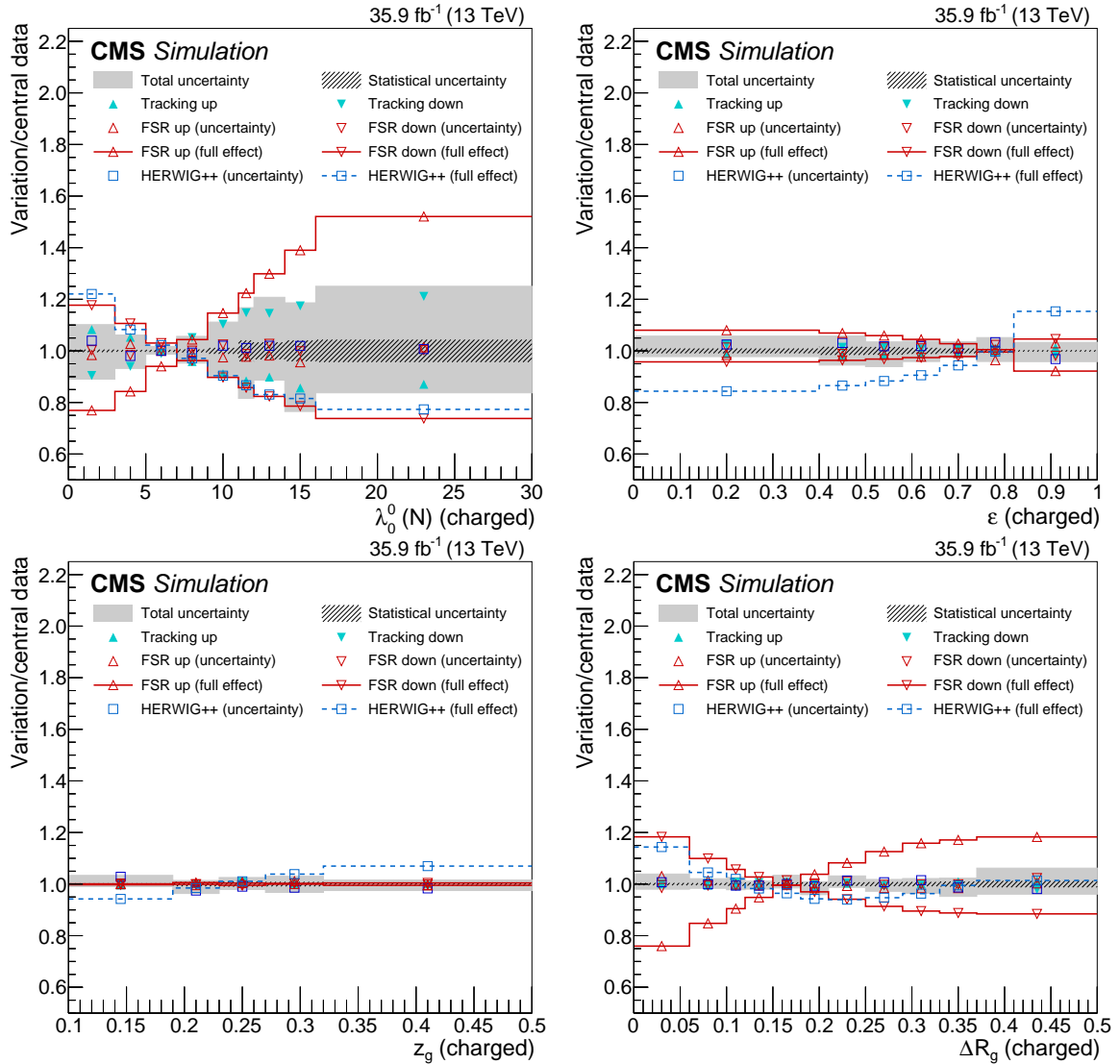
Figure 3: Systematic uncertainties for the charged multiplicity λ_0^0 (N) (upper left), jet eccentricity ε (upper right), groomed momentum fraction z_g (lower left), and angle between the groomed subjets ΔR_g (lower right). The uncertainties from FSR and HERWIG (open markers) are compared to the full effect of these variations at the particle level (open markers with lines).

6 Jet substructure observables

Jets are selected for further analysis if they satisfy $p_T > 30\,\text{GeV}$, $|\eta| < 2.0$, so that jets with $R = 0.4$ are completely contained within the tracker acceptance $|\eta| < 2.5$. Furthermore, jets are required to be separated in η–ϕ space by $\Delta R(jj) > 0.8$ to avoid overlap. The jet substructure observables are calculated from the jet constituents with $p_T > 1\,\text{GeV}$, so as to avoid the rapid decrease (increase) in tracking efficiency (misidentification rate) below $1\,\text{GeV}$ [98]. We present our results either with all (charged+neutral) particles, or with only charged particles if the resolution on the variable reconstructed from both charged+neutral particles is poor. The whole set of jet results obtained from charged and charged+neutral particles is available in the HEPDATA database [99, 100]. Hereafter, a variety of jet substructure observables are presented for the inclusive set of jets. Individual jet flavor-tagged results are shown in Section 7.
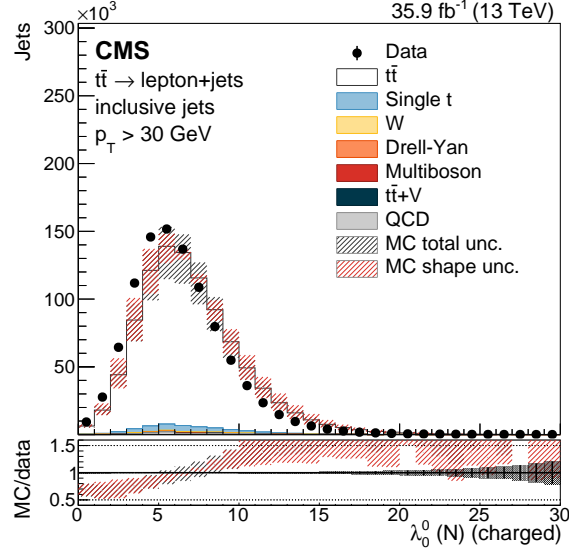
Figure 4: Charged particle multiplicity $\lambda_0^0\,(N)$ at the reconstructed level after full event selection. The lower panel shows the ratio of the MC prediction (POWHEG + PYTHIA 8) to the data (lower panels) where the black shaded band represents the statistical uncertainty on the data. The systematic uncertainties on the MC prediction are represented by hatched areas, taking into account either the total uncertainty or shape variations only.

6.1 Generalized angularities

Generalized angularities [101] are defined as

$$\lambda_\beta^\kappa = \sum_i z_i^\kappa \left(\frac{\Delta R\,(i, \hat{n}_r)}{R} \right)^\beta \tag{1}$$

where $z_i = p_T^i / \sum_j p_T^j$ is the p_T fraction carried by the particle i inside the jet, $\Delta R\,(i, \hat{n}_r)$ is its separation in η–ϕ space from the jet axis $\hat{n}_r$, $R = 0.4$ is the distance parameter used for the jet clustering, and κ and β are positive real exponents of the energy and angular weighting factors. The recoil-free jet axis $\hat{n}_r$ [102] is calculated with the "winner-takes-all" (WTA) recombination scheme [103] mitigating the impact of soft radiation. Angularities with $\kappa = 1$ are infrared- and collinear- (IRC) safe, while those with $\kappa \neq 1$ are IRC-unsafe (but "Sudakov" safe) [104]. With the exception of λ_0^0, at least two selected particles are required in the jet in order to construct these observables.

The particle multiplicity λ_0^0 is neither infrared-, nor collinear-safe, as its value is changed by additional soft emissions and/or collinear splitting of partons. In this analysis, $\lambda_0^0 = N$ (charged) is the number of charged jet constituents passing the particle p_T threshold of $1\,\text{GeV}$ and is shown at the reconstructed level in Fig. 4 and normalized and unfolded to the particle level in Fig. 5. In general, the MC generators predict a higher (integrated) charged particle multiplicity than seen in the data but the SHERPA 2 and DIRE 2 predictions achieve a fair agreement. An improved agreement could be achieved by including this or similar data in the tuning of the parton showering and hadronization [105, 106].

The jet p_T dispersion $\lambda_0^2 = p_T^d = \sum_i (p_T^i)^2 / \left(\sum_i p_T^i \right)^2$ [107] is an infrared-, but not collinear-safe quantity, highly correlated with the particle multiplicity. A scaled p_T dispersion is thus defined as

$$\lambda_0^{2*} = p_T^{d,*} = \sqrt{\left(p_T^d - \frac{1}{N} \right) \frac{N}{N-1}}; \tag{2}$$
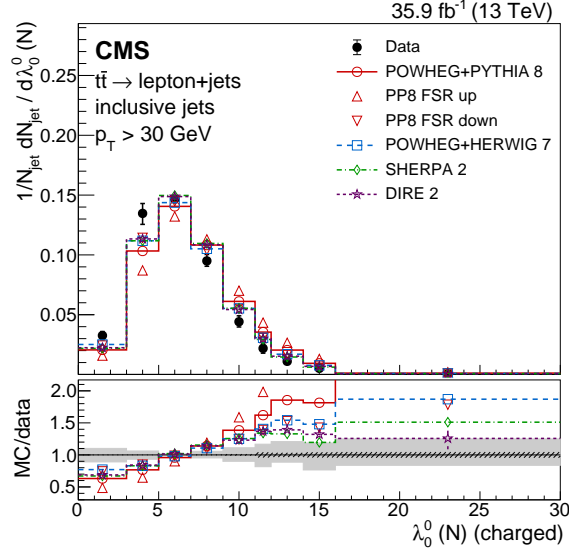
Figure 5: Charged particle multiplicity λ_0^0 (N) normalized and unfolded to the particle level, for inclusive jets. Data (points) are compared to different MC predictions (upper), and as MC/data ratios (lower). The hatched and shaded bands represent the statistical and total uncertainties, respectively.

that ensures $p_T^{d,*} \to 0$ when the p_T is equally distributed over all jet constituents, irrespective of their number, and $p_T^{d,*} \to 1$ when most of the jet momentum is carried by a single particle. The scaled p_T dispersion is shown in Fig. 6 (left) compared to the MC predictions.

The "Les Houches angularity" (LHA) $\lambda_{0.5}^1$ variable, a quantity proposed for quark-gluon discrimination [108], is well described by most available MC programs (Fig. 6, right). The high $\alpha_S^{FSR}(m_Z)$ value associated with the PYTHIA 8 FSR-up setting is disfavored.

The jet width λ_1^1, closely related to the jet broadening [109–111], is shown in Fig. 7 (left). The data favors the FSR-down variation ($\alpha_S^{FSR}(m_Z) = 0.1224$) for PYTHIA 8. The jet thrust $\lambda_2^1 \simeq m^2/E^2$ [112] is shown in Fig. 7 (right). The nominal settings of POWHEG + PYTHIA 8 and POWHEG + HERWIG 7 provide a good reproduction of the data.

For completeness, Fig. 8 shows the jet width and thrust distributions obtained using charged+neutral particles in the jet reconstruction. The comparison to the MC confirms the conclusions extracted with the charged particle-only jet reconstruction seen in Fig. 7.

6.2 Eccentricity

The eccentricity [113] is calculated as $\varepsilon = 1 - v_{\min}/v_{\max}$, where v are the eigenvalues of the energy-weighted covariance matrix M of the $\Delta\eta$ and $\Delta\phi$ distances between the jet constituents i and the WTA jet axis $\hat{n}_r$:

$$M = \sum_i E_i \begin{pmatrix} (\Delta\eta_{i,\hat{n}_r})^2 & \Delta\eta_{i,\hat{n}_r}\Delta\phi_{i,\hat{n}_r} \\ \Delta\phi_{i,\hat{n}_r}\Delta\eta_{i,\hat{n}_r} & (\Delta\phi_{i,\hat{n}_r})^2 \end{pmatrix}. \tag{3}$$

A jet perfectly circular in η–ϕ would result in $\varepsilon = 0$, while an elliptical jet gives a value $\varepsilon \to 1$. At least four particles are required in the jet to calculate the eccentricity. As shown in Fig. 9, the POWHEG + HERWIG 7 prediction agrees better with the measured distribution than the other MC programs.
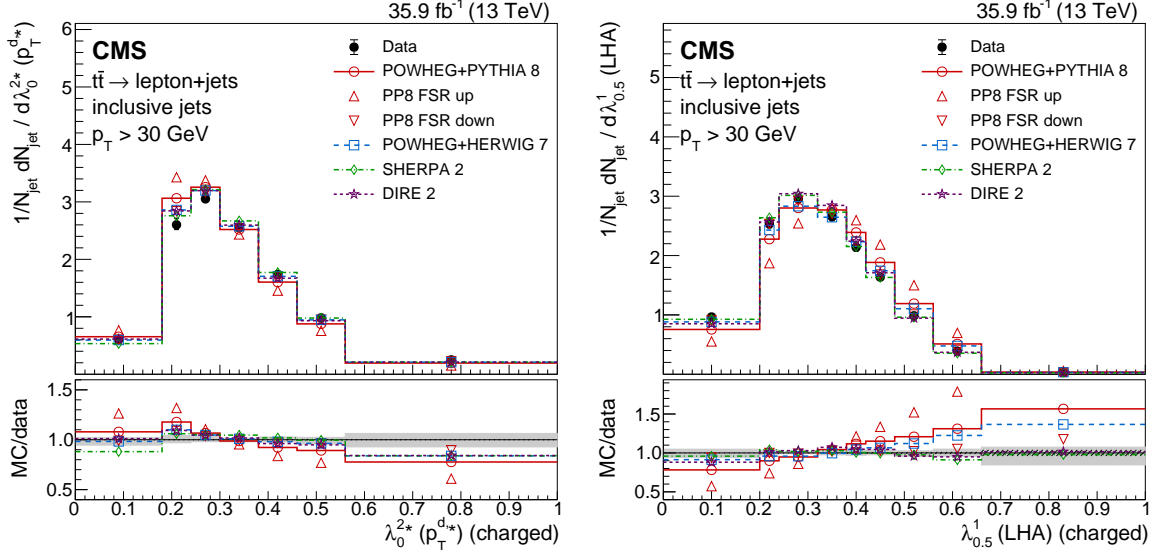
Figure 6: Distributions of the scaled p_T dispersion (λ_0^{2*}, left) and Les Houches angularity ($\lambda_{0.5}^1$, right), unfolded to the particle level, for inclusive jets reconstructed with charged particles. Data (points) are compared to different MC predictions (upper), and as MC/data ratios (lower). The hatched and shaded bands represent the statistical and total uncertainties, respectively.
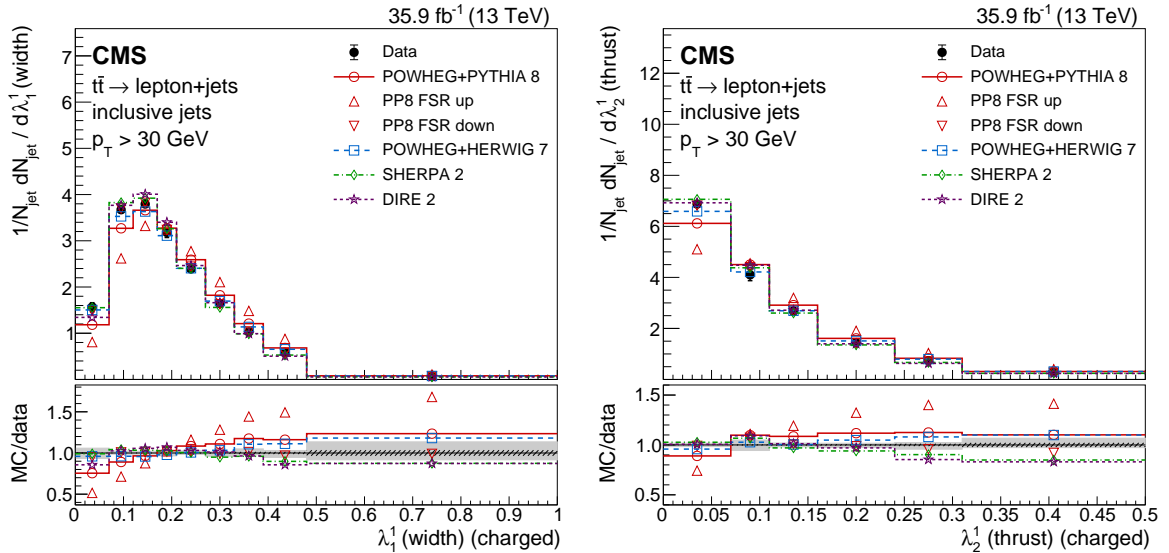

Figure 7: Distributions of the jet width (λ_1^1, left) and thrust (λ_2^1, right), unfolded to the particle level, for inclusive jets reconstructed with charged particles. Data (points) are compared to different MC predictions (upper), and as MC/data ratios (lower). The hatched and shaded bands represent the statistical and total uncertainties, respectively.
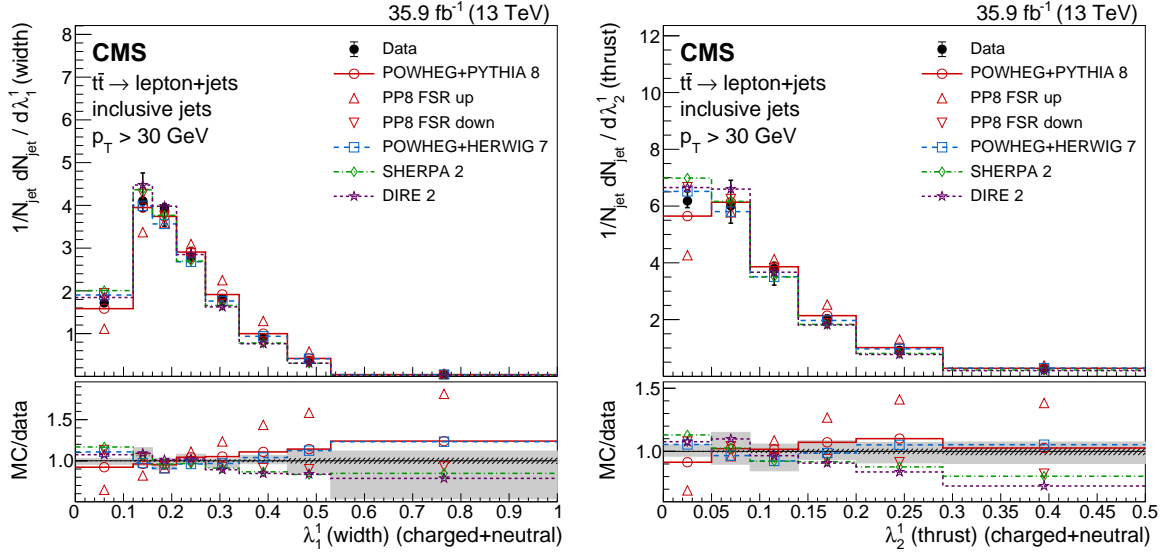
Figure 8: Distributions of the jet width (λ_1^1, left) and thrust (λ_2^1, right), unfolded to the particle level, for inclusive jets reconstructed with charged+neutral particles. Data (points) are compared to different MC predictions (upper), and as MC/data ratios (lower). The hatched and shaded bands represent the statistical and total uncertainties, respectively.
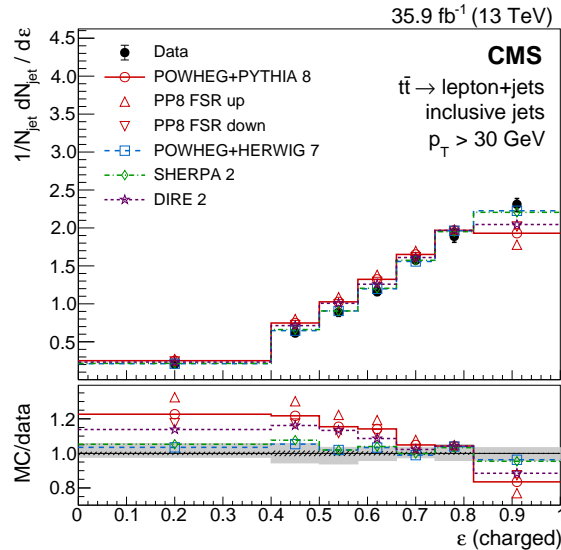

Figure 9: Distribution of the eccentricity ε, unfolded to the particle level, for inclusive jets reconstructed with charged particles. Data (points) are compared to different MC predictions (upper), and as MC/data ratios (lower). The hatched and shaded bands represent the statistical and total uncertainties, respectively.

6.3 **Soft-drop observables**

The constituents of each individual jet are first reclustered using the Cambridge–Aachen algorithm [114, 115]. The "soft-drop" (SD) algorithm [116] is then applied to remove soft, wide-angle radiation from the jet. Using the angular exponent $\beta = 0$, the soft cutoff threshold $z_{\mathrm{cut}} = 0.1$, and the characteristic parameter $R_0 = 0.4$, the SD algorithm behaves like the "modified mass drop tagger" [117]. At least two particles are required in the jet to perform soft-drop declustering.

After removing soft radiation, the groomed momentum fraction is defined as $z_{\mathrm{g}} = p_{\mathrm{T}}\left(j_2\right)/p_{\mathrm{T}}\left(j_0\right)$ of the last declustering iteration $j_0 \to j_1 + j_2$, where j_2 is the softer subjet. Such a quantity is closely related to the QCD splitting function [118], and does not depend on the value of α_S. Recently, uncorrected jet SD measurements were presented for pp collisions at 7 TeV from CMS Open Data [118], as well as in PbPb collisions at 5 TeV [119]. This analysis presents, for the first time, unfolded z_{g} distributions, shown in Fig. 10 (left). The data-model agreement is especially good for the angular-ordered shower of HERWIG 7. The angle between two groomed subjets j_1 and j_2, ΔR_{g}, is related to the jet width but also to the groomed jet area which in turn is relevant for the pileup sensitivity of the algorithm [116]. Its measured distribution is shown in Fig. 11 for both charged and charged+neutral particles, and depends strongly on the amount of FSR.

A soft-drop multiplicity [120], n_{SD}, can be defined as the number of branchings in the declustering tree that satisfy the angular cutoff $\Delta R_{\mathrm{g}} > \theta_{\mathrm{cut}}$ and

$$z_{\mathrm{g}} > z_{\mathrm{cut}}\left(\frac{\Delta R_{\mathrm{g}}}{R_0}\right)^{\beta}. \tag{4}$$

In contrast to the particle multiplicity N, n_{SD} is IRC-safe for a vast range of parameter settings, e.g., for the one used in this analysis: $z_{\mathrm{cut}} = 0.007$, $\beta = -1$, $\theta_{\mathrm{cut}} = 0$. As shown in Fig. 10 (right), the measured data distribution is higher (lower) in the data than in the MC predictions at small (large) n_{SD} values, a behavior similar to that observed for the charged multiplicity λ_0^0 (N) in Fig. 5.

6.4 $\mathcal{N}$**-subjettiness**

The $\mathcal{N}$-subjettiness $\tau_{\mathcal{N}}$ variable is constructed by first finding exactly $\mathcal{N}$ subjet seed axes using the exclusive k_{T} clustering algorithm [121] and the WTA recombination scheme. Starting from these seed axes, a local minimum of $\tau_{\mathcal{N}}$ is found, where $\tau_{\mathcal{N}}$ is calculated by summing over all particles belonging to a jet the particle p_{T} weighted by their radial distance to the nearest of the $\mathcal{N}$ candidate subjet axes:

$$\tau_{\mathcal{N}} = \frac{1}{d_0}\sum_i p_{\mathrm{T},i}\min\left\{\left(\Delta R_{1,i}\right),\left(\Delta R_{2,i}\right),\ldots,\left(\Delta R_{\mathcal{N},i}\right)\right\}, \tag{5}$$

with a normalization factor

$$d_0 = \sum_i p_{\mathrm{T},i}\left(R_0\right), \tag{6}$$

assuming the original jet distance parameter $R_0 = 0.4$.

The $\mathcal{N}$-subjettiness ratios $\tau_{\mathcal{N}\mathcal{M}} = \tau_{\mathcal{N}}/\tau_{\mathcal{M}}$, defined in [122, 123], were shown to be especially useful for distinguishing jets with $\mathcal{N}$ or $\mathcal{M}$ subjets. In this analysis, τ_{21}, τ_{32}, and τ_{43} are measured, which are frequently used in the identification of heavy Lorentz-boosted objects. At least $\mathcal{N} + 1$ particles are required in the jet to calculate these observables. As shown in Figs. 12 and 13, the measured $\tau_{\mathcal{N}\mathcal{M}}$ distributions are consistently shifted to lower values than those
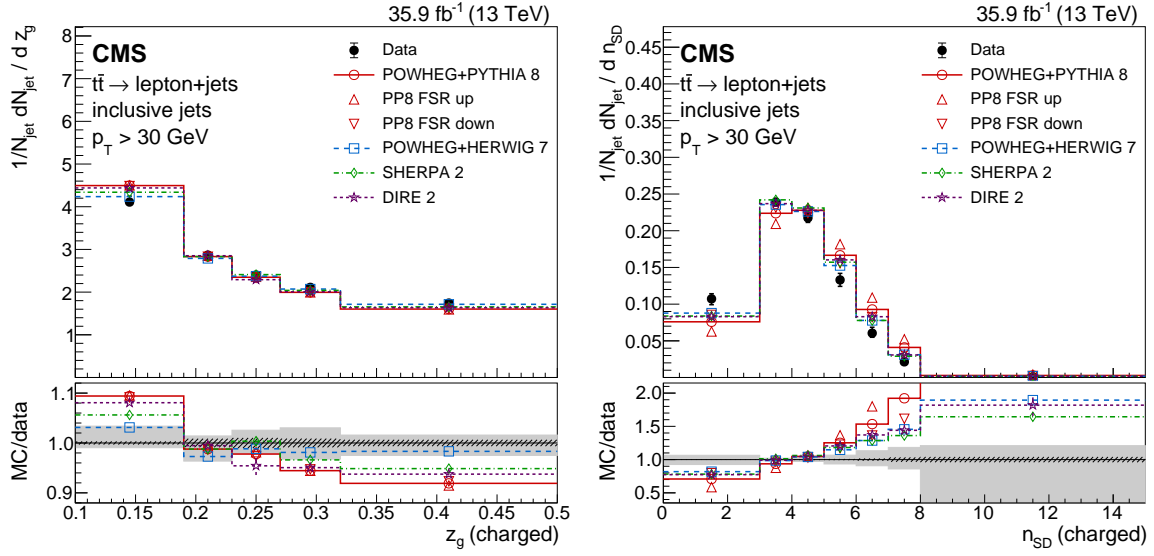
Figure 10: Distributions of the groomed momentum fraction z_g (left) and the soft-drop multiplicity n_{SD} (right), unfolded to the particle level, for inclusive jets reconstructed with charged particles. Data (points) are compared to different MC predictions (upper), and as MC/data ratios (lower). The hatched and shaded bands represent the statistical and total uncertainties, respectively.
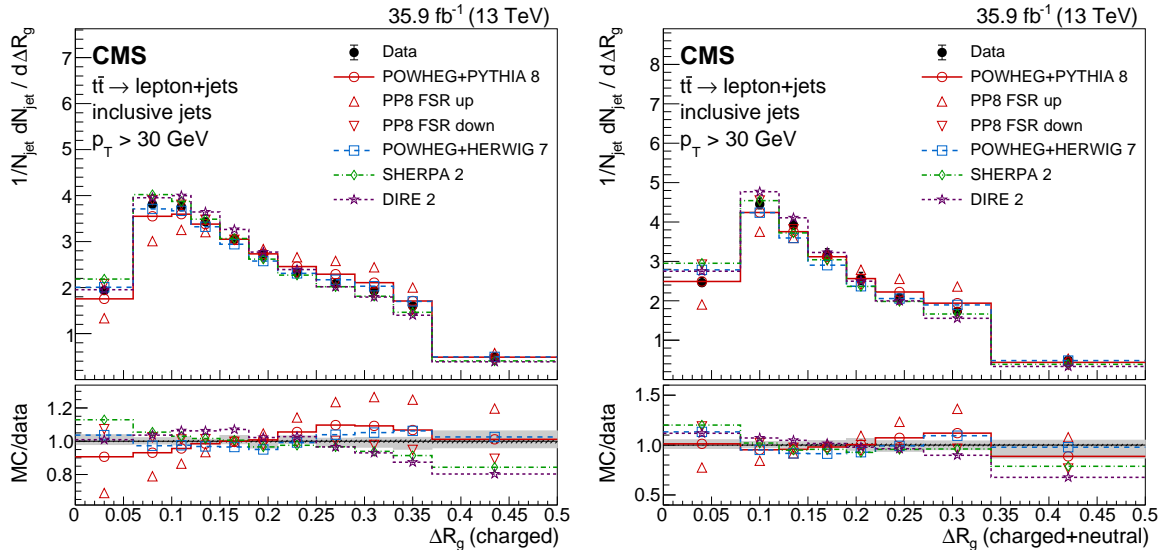

Figure 11: Distributions of the angle between the groomed subjets ΔR_g, unfolded to the particle level, for inclusive jets reconstructed with charged (left) and charged+neutral particles (right). Data (points) are compared to different MC predictions (upper), and as MC/data ratios (lower). The hatched and shaded bands represent the statistical and total uncertainties, respectively.
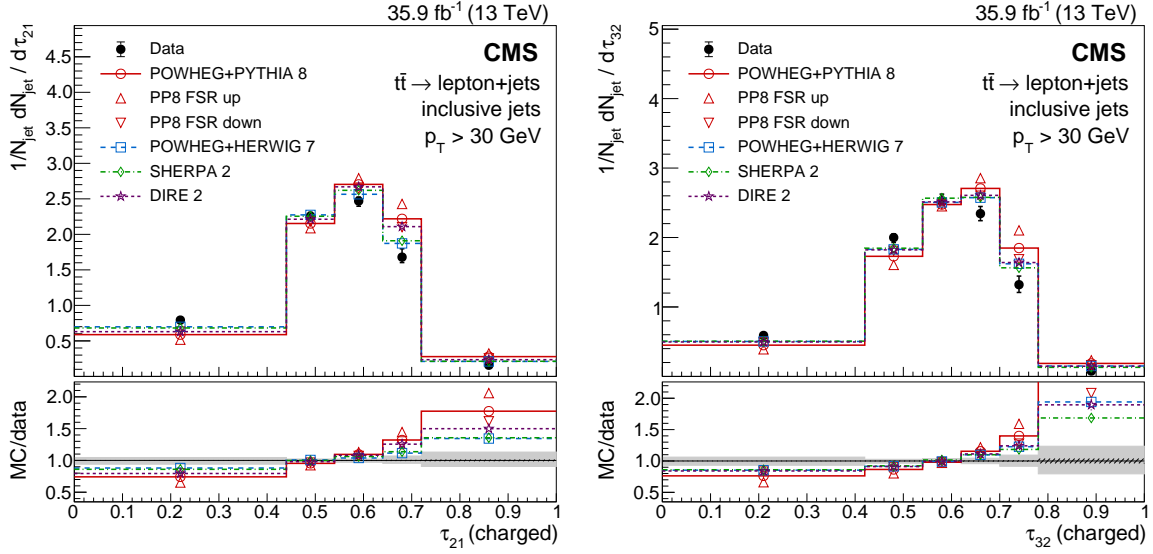
Figure 12: Distributions of the $\mathcal{N}$-subjettiness ratios τ_{21} (left) and τ_{32} (right), unfolded to the particle level, for inclusive jets reconstructed with charged particles. Data (points) are compared to different MC predictions (upper), and as MC/data ratios (lower). The hatched and shaded bands represent the statistical and total uncertainties, respectively.

predicted by the MC programs. While the expectation from boosted object studies is that $\mathcal{N}$-prong ($\mathcal{M}$-prong) jets acquire a lower (higher) value of $\tau_{\mathcal{N}\mathcal{M}}$, the behavior of $\tau_{\mathcal{N}\mathcal{M}}$ in a resolved topology seems to be mainly driven by the particle multiplicity.

6.5 Energy correlation functions

The $\mathcal{N}$-point energy correlation double ratios $C_{\mathcal{N}}^{(\beta)}$ [124] are defined as

$$C_{\mathcal{N}}^{(\beta)} = \frac{\text{ECF}\left(\mathcal{N}+1, \beta\right) \text{ECF}\left(\mathcal{N}-1, \beta\right)}{\text{ECF}\left(\mathcal{N}, \beta\right)^2}, \tag{7}$$

where

$$\text{ECF}\left(\mathcal{N}, \beta\right) = \sum_{i_1 < i_2 < \ldots < i_{\mathcal{N}} \in j} \left(\prod_{a=1}^{\mathcal{N}} p_{T_{i_a}}\right) \left(\prod_{b=1}^{\mathcal{N}-1} \prod_{c=b+1}^{\mathcal{N}} \Delta R_{i_b i_c}\right)^{\beta}$$

and the sum runs over the constituents i of the jet j with their p_T product being multiplied with the pairwise distances $\Delta R_{i_b i_c}$ in η–ϕ space. Each $C_{\mathcal{N}}$ is sensitive to the $(\mathcal{N}-1)$-prong substructure of the jet, while the angular exponent β adjusts the sensitivity to near-collinear splittings. At least $\mathcal{N}+1$ particles are required in the jet to calculate these observables. In this analysis, parameter values $\mathcal{N} = \{1, 2, 3\}$ and $\beta = \{0, 0.2, 0.5, 1, 2\}$ are investigated. The distributions for each $\mathcal{N}$ and $\beta = \{0, 1\}$ are shown in Figs. 14–16. For $\beta > 0$ the observable is IRC-safe and the data are better described by the MC generators than for $\beta = 0$. Many observables of this family show significant differences between the jet flavors, as shown later in Fig. 19 (bottom, right).

More recently, the M_i and N_i series observables [125] were proposed as the following ratios of generalized energy correlation functions:

$$M_i^{(\beta)} = \frac{_1e_{i+1}^{(\beta)}}{_1e_i^{(\beta)}}, \quad N_i^{(\beta)} = \frac{_2e_{i+1}^{(\beta)}}{\left(_1e_i^{(\beta)}\right)^2}, \tag{8}$$
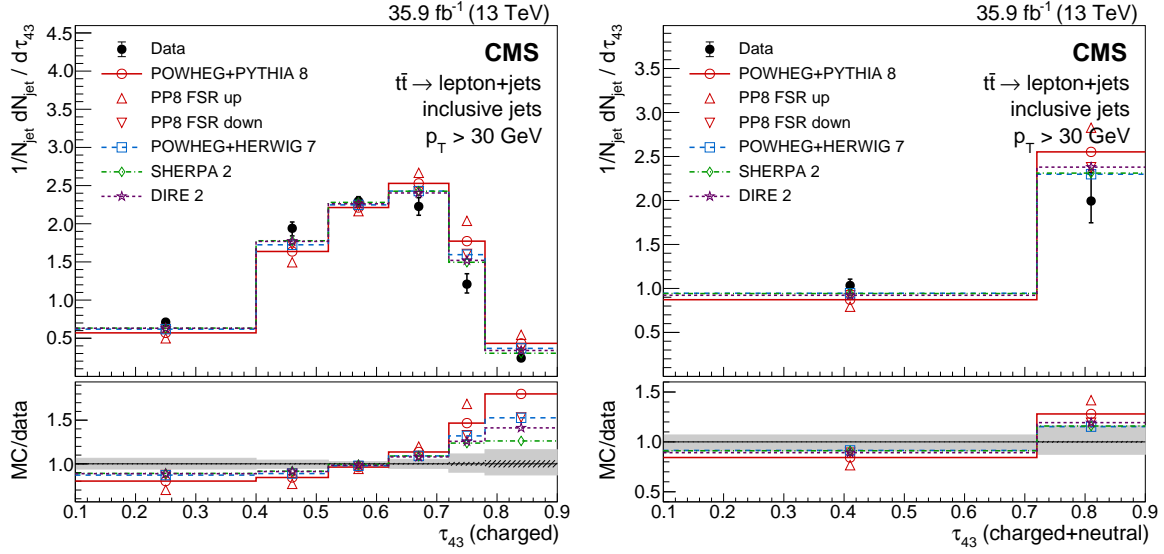
Figure 13: Distributions of the $\mathcal{N}$-subjettiness ratio τ_{43}, unfolded to the particle level, for inclusive jets reconstructed with charged (left) and charged+neutral particles (right). Data (points) are compared to different MC predictions (upper), and as MC/data ratios (lower). The hatched and shaded bands represent the statistical and total uncertainties, respectively.

where

$$
{}_v e_n^{(\beta)} = \sum_{1 \leq i_1 < i_2 < \cdots < i_n \in j} z_{i_1} z_{i_2} \ldots z_{i_n} \prod_{m=1}^{v} \min_{s < t \in \{i_1, i_2, \ldots, i_n\}}^{(m)} \left\{ \Delta R_{st}^{\beta} \right\}
$$

and the sum runs over all particles i in the jet j with p_T fractions z_i, $\min^{(m)}$ denotes the m-th smallest angular distance, n is the number of particles to be correlated, v denotes the number of pairwise angles entering the product, and β is the angular exponent. The observables are Lorentz invariant under boosts along the jet axis and IRC-safe for $\beta > 0$. The distributions of M_2, N_2, and N_3 have been measured for $\beta = \{1,2\}$. Figures 17 and 18 show the results for $\beta = 1$. The POWHEG + HERWIG 7 prediction describes these data better than the other MC generators.

7 Jet substructure for different jet flavors

All jet substructure observables have been measured not only for inclusive jets, but also for b quark jets, and for samples enriched in light-quark or gluon jets, respectively. The flavor categories are defined as follows below. The relative contributions to the inclusive jet sample at the particle level are obtained from the default POWHEG + PYTHIA 8 simulation with little dependence on the generator. The parton flavor (quarks and gluons) is determined from the leading p_T parton that can be associated with a jet in POWHEG + PYTHIA 8 simulation. It should be noted that the parton information is very generator-dependent and only serves for illustration of the level of purity of the light- and gluon-enriched samples.

Bottom quark jets (44% of the inclusive jet sample)

At detector level, jets are identified as b-tagged by the CSVv2 algorithm. At particle level, at least one b hadron is required to be clustered in the jet.

These jets originate from b quarks in more than 99% of the cases. No distinction is made between b jets from the top quark decay and additional b jets from gluon splitting.
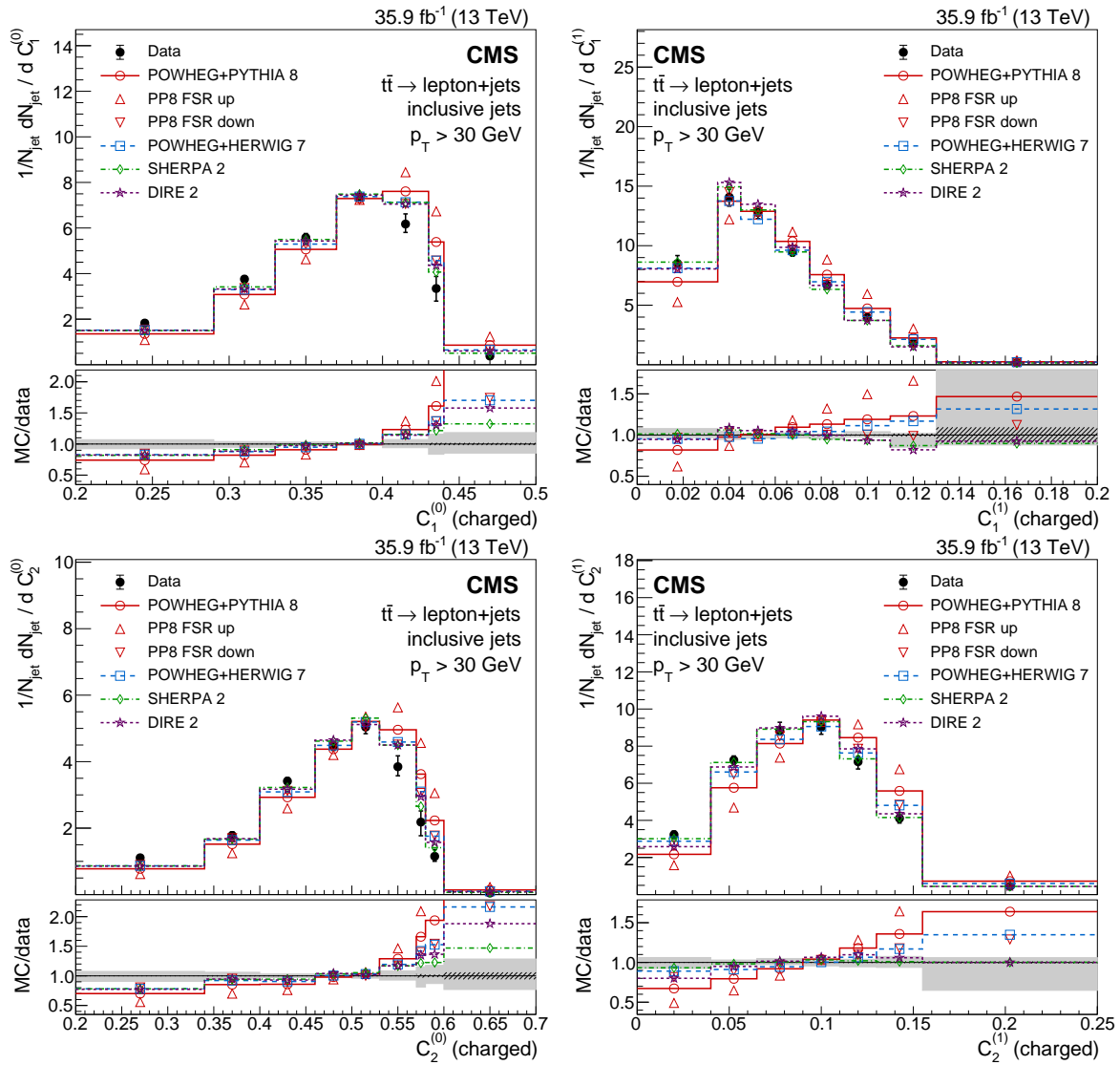
Figure 14: Distributions of energy correlation ratios $C_1^{(0)}$ (upper left), $C_1^{(1)}$ (upper right), $C_2^{(0)}$ (lower left) and $C_2^{(1)}$ (lower right), unfolded to the particle level, for inclusive jets reconstructed with charged particles. Data (points) are compared to different MC predictions (upper), and as MC/data ratios (lower). The hatched and shaded bands represent the statistical and total uncertainties, respectively.
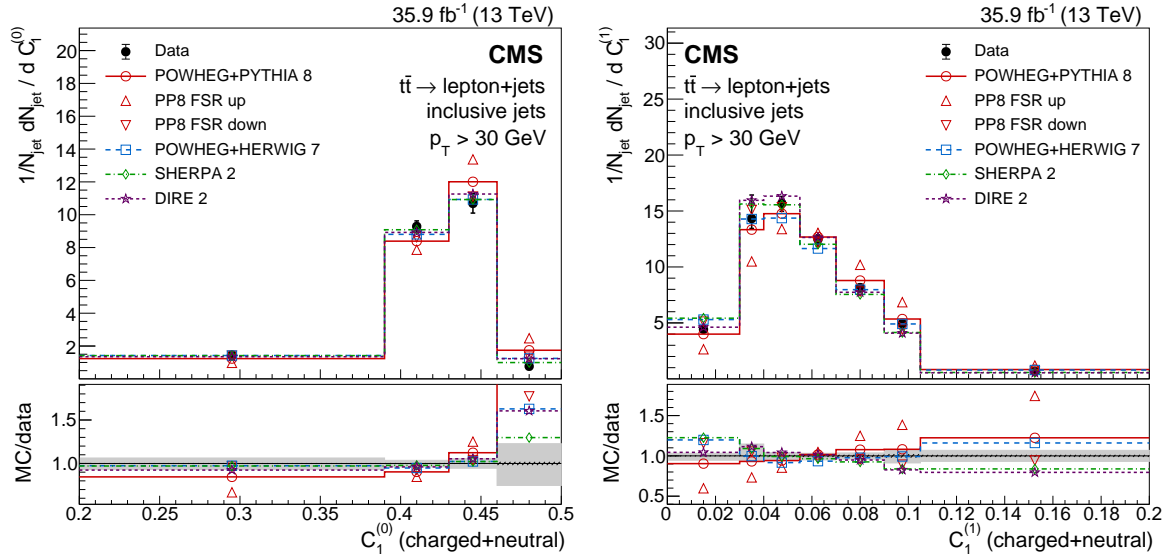
Figure 15: Distributions of energy correlation ratios $C_1^{(0)}$ (left) and $C_1^{(1)}$ (right), unfolded to the particle level, for inclusive jets reconstructed with charged+neutral particles. Data (points) are compared to different MC predictions (upper), and as MC/data ratios (lower). The hatched and shaded bands represent the statistical and total uncertainties, respectively.
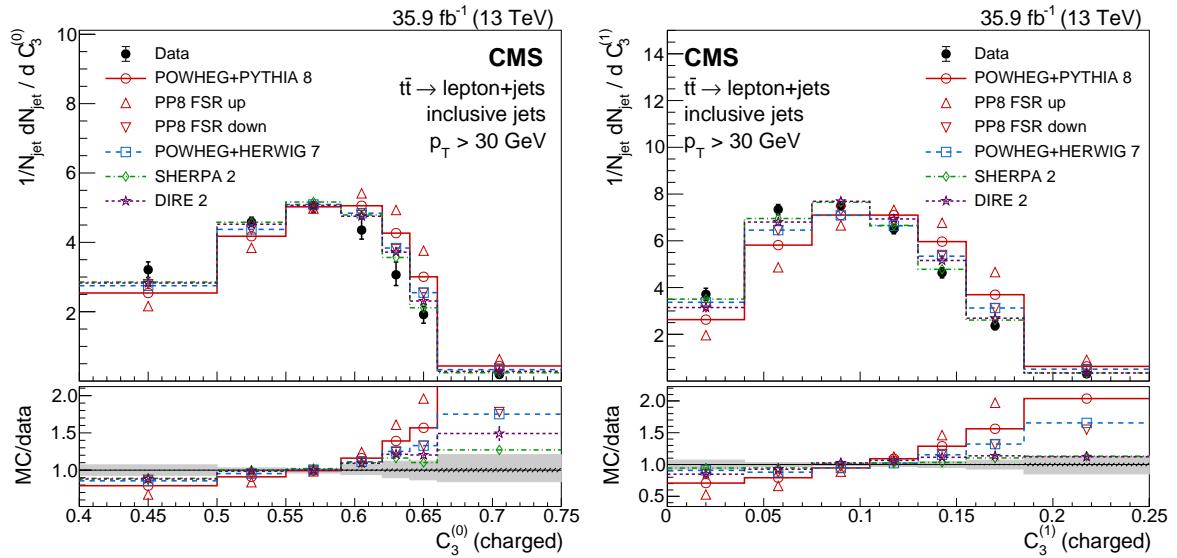

Figure 16: Distributions of energy correlation ratios $C_3^{(0)}$ (left) and $C_3^{(1)}$ (right), unfolded to the particle level, for inclusive jets reconstructed with charged particles. Data (points) are compared to different MC predictions (upper), and as MC/data ratios (lower). The hatched and shaded bands represent the statistical and total uncertainties, respectively.
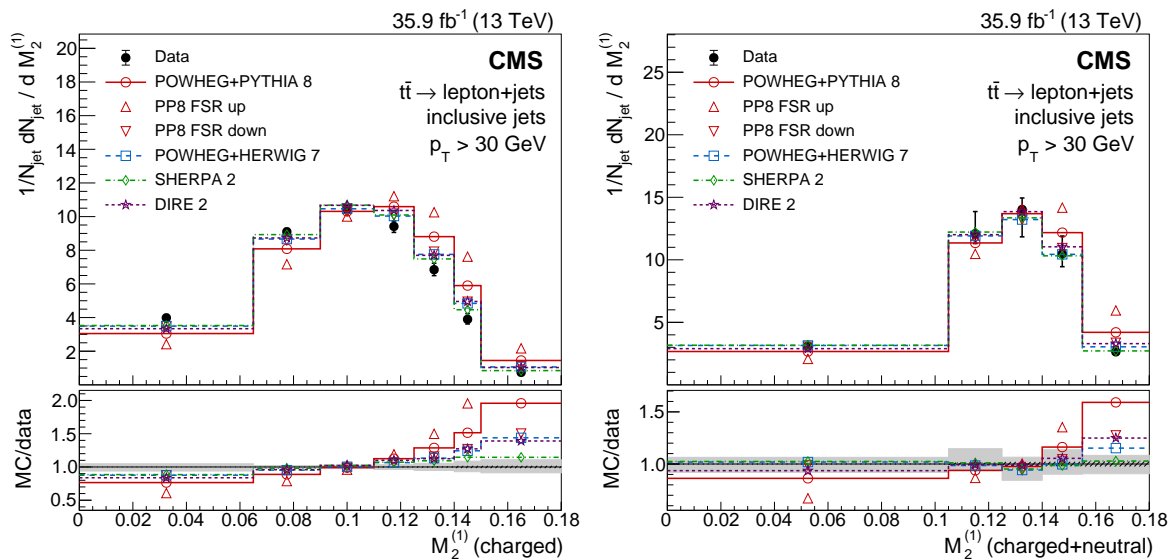
Figure 17: Distributions of the energy correlation ratio $M_2^{(1)}$, unfolded to the particle level, for inclusive jets reconstructed with charged (left) or charged+neutral particles (right). Data (points) are compared to different MC predictions (upper), and as MC/data ratios (lower). The hatched and shaded bands represent the statistical and total uncertainties, respectively.
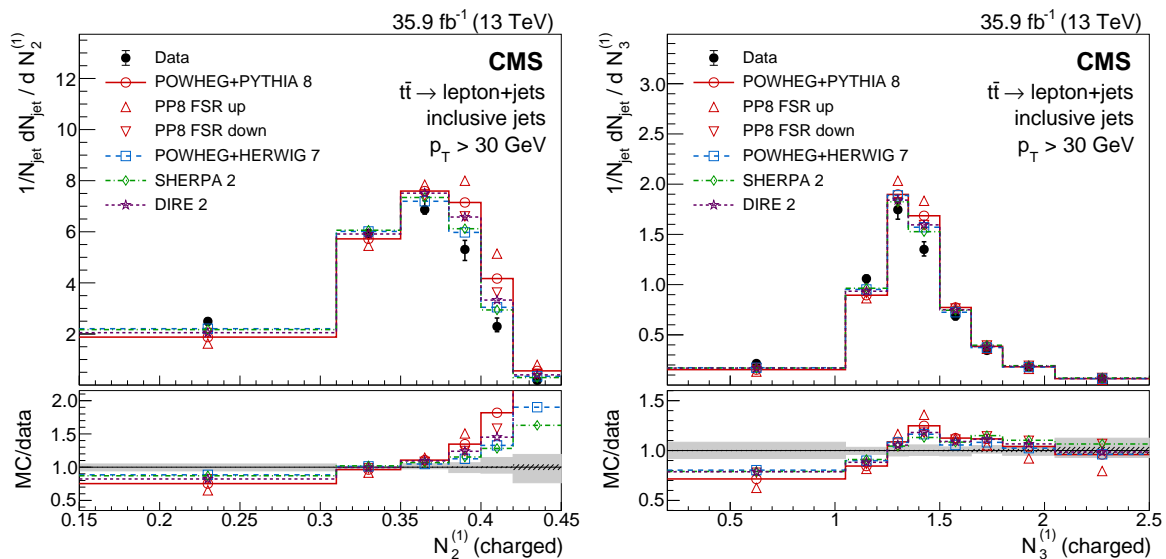

Figure 18: Distribution of the energy correlation ratios $N_2^{(1)}$ (left) and $N_3^{(1)}$ (right), unfolded to the particle level, for inclusive jets reconstructed with charged particles. Data (points) are compared to different MC predictions (upper), and as MC/data ratios (lower). The hatched and shaded bands represent the statistical and total uncertainties, respectively.

Light-quark jets (46% of the inclusive jet sample)
Jets are assigned to the light-quark-enriched jet sample if they are not b-tagged and are paired with another similar jet to give a W boson candidate with an invariant mass satisfying $|m_{jj} - 80.4\,\text{GeV}| < 15\,\text{GeV}$. Of these jets, 50% stem from light quarks, 21% from charm quarks, and 29% from gluons.

Gluon jets (10% of the inclusive jet sample)
A sample enriched in gluon jets is obtained by selecting jets that are neither b-tagged nor associated to a W boson candidate, but instead are likely to originate from ISR. This sample is composed of jets stemming from bottom (1%), charm (11%), and light quarks (31%), and gluons (58%).

Observables relevant for studies of quark/gluon discrimination, such as the charged multiplicity, scaled p_T dispersion, Les Houches angularity, and the energy correlation ratio $C_3^{(1)}$ are shown in Fig. 19 for the three exclusive jet samples. For all observables, the differences between the quark- and gluon-enriched samples do not seem to be very strong, with the energy correlation ratio $C_3^{(1)}$ providing the best separation. This might be caused by the algorithmic definition of the samples that leads to a high contamination with other partonic flavors. It is notable that the data/MC agreement for bottom-quark jets is significantly worse than for the light- and gluon-enriched samples, see also the χ^2 tests in Section 8. Therefore, an update in the MC parameter tuning and/or physics modeling may require flavor-dependent improvements to match the data.

8   Compatibility tests with minimally correlated observables

The compatibility of the unfolded data and different MC predictions is tested by calculating $\chi^2 = \Delta^T C^{-1} \Delta$, where $\Delta = (\vec{x}_\text{data} - \vec{x}_\text{MC})$ is the vector of measurement residuals, and C is the total covariance matrix of the measurement, given by $C = C_\text{stat} + \sum_\text{syst} C_\text{syst}$, with the vector/matrix entries for the first bin removed to make C invertible.

The statistical covariance matrices C_stat for the normalized distributions are obtained from 1000 pseudo-experiments per observable. For uncertainties described by a single systematic shift, the systematic covariance matrix is defined as $C_\text{syst}(i, j) = \left(x_i^\text{syst} - x_i^\text{nom} \right) \left(x_j^\text{syst} - x_j^\text{nom} \right)$, where x_i^nom is the vector representing the nominal result. For uncertainties described by two opposite shifts, the systematic covariance matrix is defined as

$$
\begin{aligned}
C_\text{syst}(i, j) = {} & \max\left(|x_i^\text{syst+} - x_i^\text{nom}|, |x_i^\text{syst-} - x_i^\text{nom}| \right) \\
& \times \max\left(|x_j^\text{syst+} - x_j^\text{nom}|, |x_j^\text{syst-} - x_j^\text{nom}| \right) \\
& \times \text{sign}\left(\left[x_i^\text{syst+} - x_i^\text{syst-} \right] \left[x_j^\text{syst+} - x_j^\text{syst-} \right] \right),
\end{aligned}
$$

which corresponds to symmetrizing the largest observed shift in each bin.

By construction, the considered jet-substructure observables exhibit significant correlation with each other, as shown by the pair-wise sample Pearson correlation coefficients in Figs. 20 and 21. For further analysis, it is useful to identify a subset of observables with low correlation to each other.

A suitable subset of 4 observables is identified that have an absolute correlation of less than 30% among each other: the charged multiplicity $\lambda_0^0 (N)$, the eccentricity ε, the groomed momentum
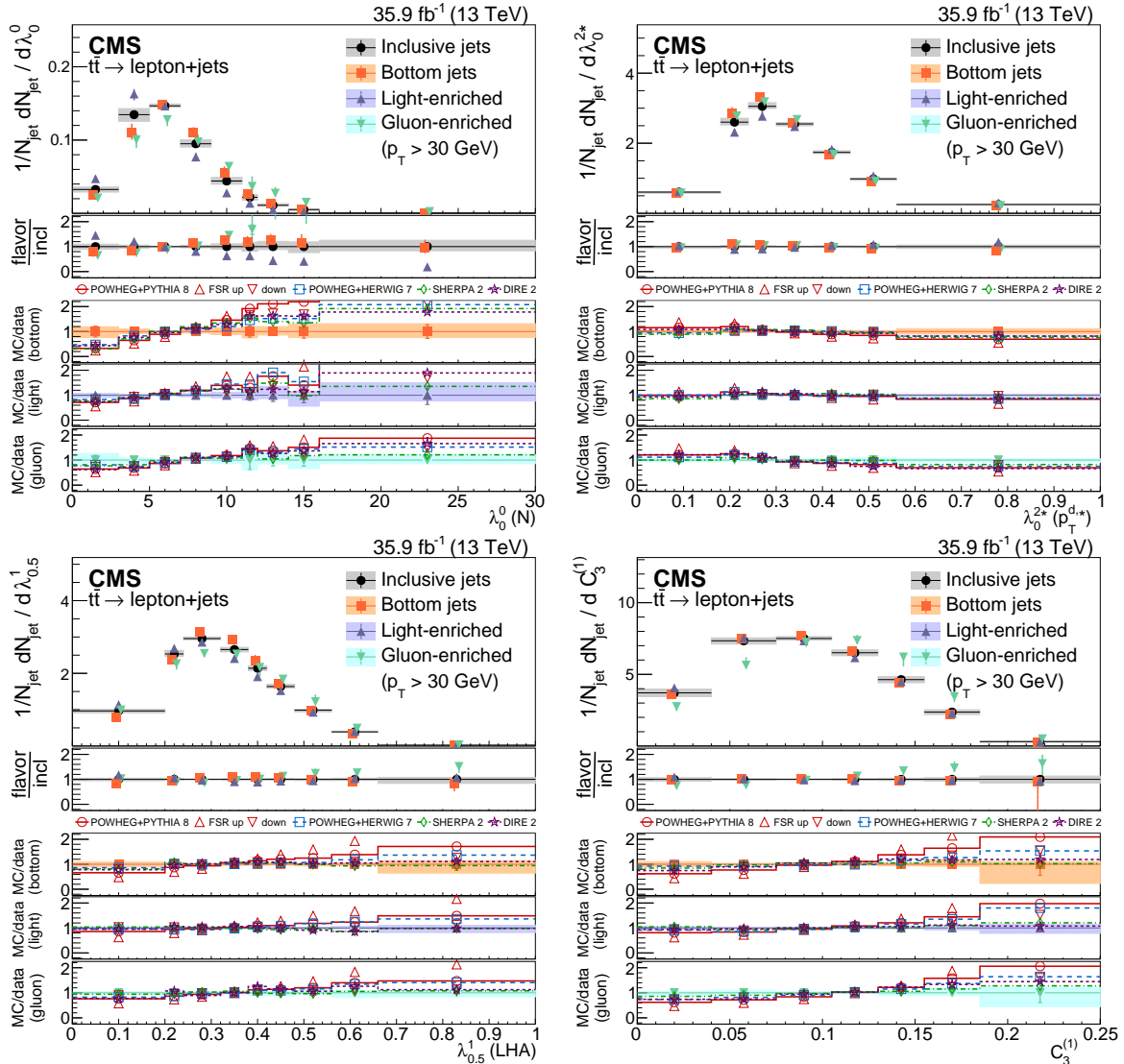
Figure 19: Distributions of the charged multiplicity (upper left), scaled p_T dispersion (λ_0^{2*}) (upper right), Les Houches angularity ($\lambda_{0.5}^1$) (lower left), and the energy correlation ratio $C_3^{(1)}$ (lower right), unfolded to the particle level, for jets of different flavors. The second panel shows the corresponding ratios of the different flavors over the inclusive jets data. The sub-panels show the ratios of the different MC predictions over the bottom, light-quark-enriched, and gluon-enriched jet data.
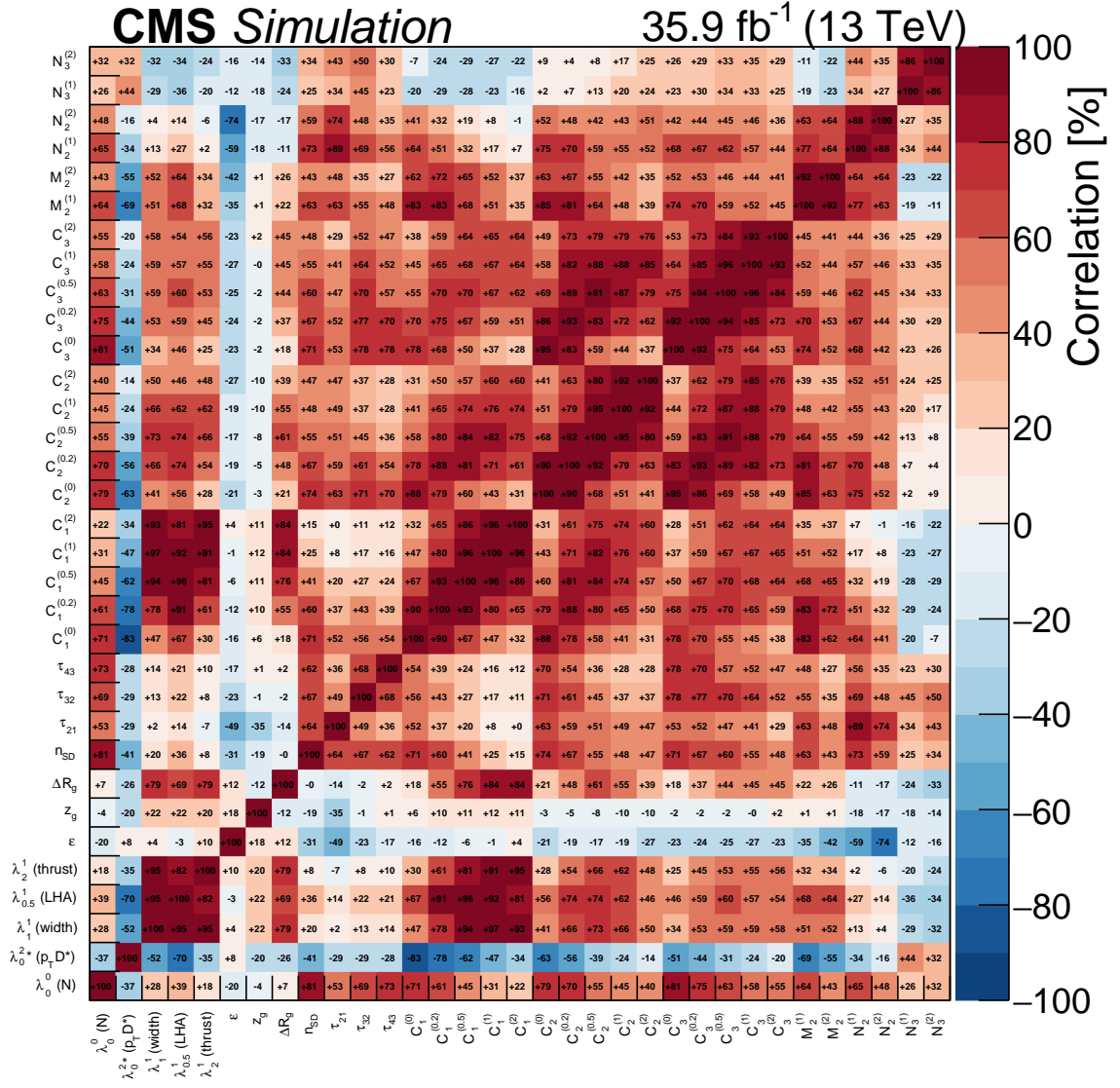
Figure 20: Correlations of the jet-substructure observables used in this analysis obtained at the particle level.
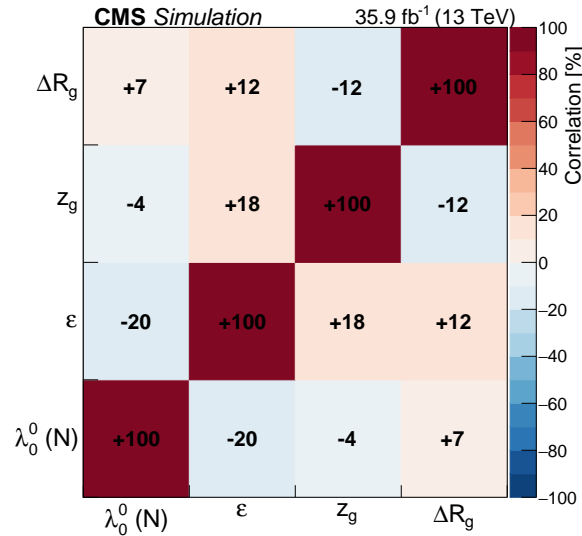
Figure 21: Correlations of the jet-substructure observables used in this analysis obtained at the particle level for the set of four minimally correlated observables.

fraction z_g, and the angle between the groomed subjets ΔR_g. The associated data-to-simulation goodness-of-fit values, χ^2, for these four low-correlation observables are listed in Tables 2 and 3.

Among the POWHEG + PYTHIA 8 predictions, the FSR-down setting with $\alpha_S^{\text{FSR}}(m_Z) = 0.1224$ shows improved agreement with data, except for z_g which does not depend on the value of $\alpha_S^{\text{FSR}}(m_Z)$. The agreement with data is also improved by the alternative models for CR and by the rope hadronization model [126]. The ΔR_g observable is also shown to be sensitive to the b fragmentation function, and shows better agreement with harder fragmentation. The agreement of the POWHEG + PYTHIA 8 predictions with the jet eccentricity data is poor compared to SHERPA 2 and POWHEG + HERWIG 7, particularly. The POWHEG + HERWIG 7 generator setup with the angular-ordered shower also provides the best description of the groomed momentum fraction z_g. The prediction by SHERPA 2 has an overall good agreement with the data, but does not describe well the ΔR_g of bottom-quark jets. This might be caused by the missing ME corrections to the radiation from the b quark in the top quark decay.

9 Extraction of the strong coupling

The value of the strong coupling preferred by the jet substructure observables can be extracted from a comparison of the measured distributions to POWHEG + PYTHIA 8 predictions. Monte Carlo samples were generated with $\alpha_S^{\text{FSR}}(m_Z)$ values between 0.08 and 0.14, where higher-order corrections to soft gluon emissions are incorporated in an effective way using 2-loop running of the strong coupling and CMW rescaling [62]. The χ^2 scan of $\alpha_S^{\text{FSR}}(m_Z)$ for the low-correlation observables is shown in Fig. 22. The charged multiplicity and the jet eccentricity are sensitive to $\alpha_S^{\text{FSR}}(m_Z)$ but are expected to be highly affected by the modeling of nonperturbative effects, pointing to the need of tuning additional parameters. As expected, the groomed momentum fraction z_g is independent of $\alpha_S^{\text{FSR}}(m_Z)$.

The angle between the groomed subjets, ΔR_g, is measured with high precision and the removal of soft radiation lowers the impact of nonperturbative effects. The value of $\alpha_S(m_Z)$ can be extracted from this observable with an experimental uncertainty of ±0.001 using the b jet sample

Table 2: χ^2 values and the numbers of degrees of freedom (ndf) for the data-to-simulation comparison of the distributions of the four weakly-correlated jet substructure observables, λ_0^0 (N), ε, z_g, and ΔR_g, for four different jet flavors and six MC generator setups.

		POWHEG + PYTHIA 8			POWHEG + HERWIG 7	SHERPA 2	DIRE 2
		FSR-down	Nominal	FSR-up			
$\alpha_S^{\text{FSR}}(m_Z)$		0.1224 One-loop	0.1365 One-loop	0.1543 One-loop	0.1262 Two-loop	0.118 Two-loop CMW	0.1201 Two-loop
Observable	Flavor	χ^2	χ^2	χ^2	χ^2	χ^2	χ^2
λ_0^0 (N) ndf = 8	Inclusive	23.4	88.0	390.5	27.4	16.1	15.1
	Bottom	35.7	110.6	432.9	35.4	20.0	26.0
	Light	7.2	12.3	53.3	24.5	13.2	24.0
	Gluon	9.0	26.1	84.5	13.5	4.7	14.1
ε ndf = 6	Inclusive	72.6	108.8	217.6	6.3	9.4	61.6
	Bottom	28.2	48.7	102.9	2.1	4.8	21.7
	Light	27.6	44.6	89.6	3.9	2.7	26.3
	Gluon	57.0	81.3	133.4	7.5	19.7	73.6
z_g ndf = 4	Inclusive	18.9	20.7	23.2	1.8	7.7	16.2
	Bottom	4.8	6.4	8.6	1.2	1.5	3.0
	Light	22.0	20.7	19.5	1.3	8.9	27.6
	Gluon	11.2	10.4	8.8	2.0	9.6	15.9
ΔR_g ndf = 10	Inclusive	19.5	29.3	241.5	23.2	41.8	77.0
	Bottom	23.2	18.4	227.5	16.6	79.1	15.8
	Light	9.3	29.3	251.0	120.1	40.2	221.6
	Gluon	11.7	8.6	69.5	19.7	28.3	33.1

Table 3: χ^2 values and the numbers of degrees of freedom (ndf) for the data-to-simulation comparison of the distributions of the four weakly-correlated jet substructure observables, $\lambda_0^0\,(N)$, ε, z_g, and ΔR_g, for four different jet flavors and seven POWHEG + PYTHIA 8 model variations. The value of the strong coupling is $\alpha_S^{\mathrm{FSR}}(m_Z) = 0.1365$ for all predictions.

| | | Nominal | CR/hadronization | | | b fragmentation | | |
| | | | QCD | Move | Rope | Soft | Hard | Peterson |
Observable	Flavor	χ^2	χ^2	χ^2	χ^2	χ^2	χ^2	χ^2
$\lambda_0^0\,(N)$ ndf = 8	Inclusive	88.0	42.1	57.0	51.6	120.7	78.5	158.7
	Bottom	110.6	80.1	95.7	65.4	159.3	96.4	207.6
	Light	12.3	9.5	12.3	10.3	12.6	12.1	12.6
	Gluon	26.1	7.4	13.0	21.5	27.4	25.5	27.5
ε ndf = 6	Inclusive	108.8	85.3	89.5	94.6	118.6	103.3	108.5
	Bottom	48.7	44.0	45.7	37.4	56.7	44.3	48.5
	Light	44.6	32.1	34.5	42.0	45.7	44.0	45.4
	Gluon	81.3	40.4	54.7	87.9	81.8	80.9	81.1
z_g ndf = 4	Inclusive	20.7	15.6	18.5	18.0	22.3	19.5	18.1
	Bottom	6.4	6.0	5.8	5.2	7.3	5.7	4.8
	Light	20.7	14.8	18.9	18.8	20.8	20.7	20.7
	Gluon	10.4	6.1	8.6	9.8	10.5	10.4	10.4
ΔR_g ndf = 10	Inclusive	29.3	24.8	26.1	23.7	48.2	23.2	44.7
	Bottom	18.4	18.6	15.8	9.1	60.1	8.6	55.4
	Light	29.3	18.5	23.5	18.4	33.6	27.2	32.7
	Gluon	8.6	4.7	7.6	9.0	8.6	8.6	8.3

(Fig. 22, right). These bottom-quark jets stem mostly from top quark decays where the PYTHIA 8 prediction incorporates ME corrections, describing the jet substructure at LO accuracy in the hard emission limit, while also being at least LL accurate elsewhere. The modeling uncertainties are estimated by the POWHEG + PYTHIA 8 variations described in Section 5, as well as by a comparison to the results obtained with the rope hadronization model. This extraction of $\alpha_S(m_Z)$ is currently limited by the FSR scale uncertainties of $^{+0.014}_{-0.012}$. Other relevant model uncertainties stem from the b fragmentation ($^{+0.003}_{-0.006}$) and the alternative rope hadronization model (+0.002). Taking into account all uncertainties, a value of $\alpha_S(m_Z) = 0.115^{+0.015}_{-0.013}$ is obtained from the b jet sample. An extraction using charged+neutral particles leads to an identical result even though with a slightly larger experimental uncertainty of ± 0.002.

The default POWHEG + PYTHIA 8 samples were generated without CMW rescaling and with first-order running of α_S. In this case, a value of $\alpha_S(m_Z) = 0.130^{+0.016}_{-0.020}$ is extracted from the b jet sample. This value is in between those of the POWHEG + PYTHIA 8 nominal sample with $\alpha_S^{FSR}(m_Z) = 0.1365$ and the "FSR down" sample which has an effective $\alpha_S^{FSR}(m_Z) = 0.1224$ for final-state radiation. A lower value of $\alpha_S^{FSR}(m_Z)$ also improves the data-to-simulation agrement for charged multiplicity and jet eccentricity although some discrepancy remains.
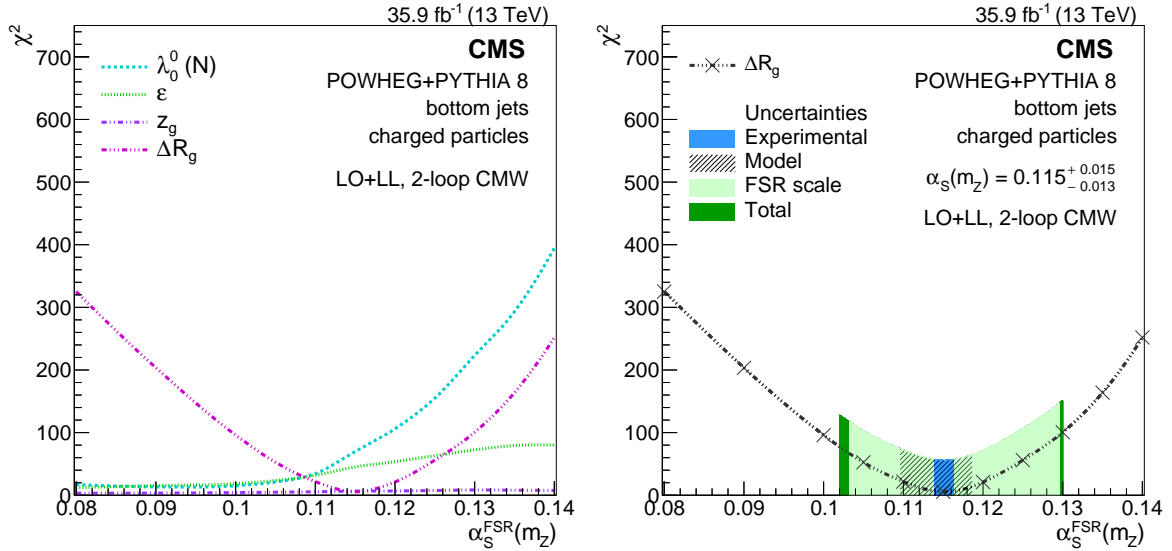

Figure 22: Scans of χ^2 as a function of $\alpha_S^{FSR}(m_Z)$, derived from the bottom-quark jet sample, for the minimally-correlated observables $\lambda_0^0(N)$, ε, z_g, and ΔR_g (left), and for ΔR_g alone with uncertainties indicated by the shaded areas (right).

10   Summary

A measurement of jet substructure observables in resolved $t\bar{t}$ lepton+jets events from pp collisions at $\sqrt{s} = 13$ TeV has been presented, including several variables relevant for quark-gluon discrimination and for heavy Lorentz-boosted object identification. The investigated observables provide valuable insights on the perturbative and nonperturbative phases of jet evolution. Their unfolded distributions have been derived for inclusive jets, as well as for samples enriched in jets originating from bottom quarks, light quarks, or gluons.

Data are compared to theoretical predictions either based on next-to-leading-order (NLO) matrix-element calculations (POWHEG) interfaced with different generators for the parton shower and hadronization (either PYTHIA 8 or HERWIG 7), or based on SHERPA 2 with NLO corrections, as

well as on the DIRE 2 shower model. The correlations between all jet substructure variables have been studied. Eliminating observables with a high level of correlation, a set of four variables is identified and used for quantifying the level of data-simulation agreement. With the default Monte Carlo (MC) generator tunes, none of the predictions yields a good overall reproduction of the experimental distributions. Thus, some further tuning of the models is required, with special attention to the data/MC disagreement observed in the particle multiplicity λ_0^0 and correlated observables, including those designed for quark/gluon discrimination. The groomed momentum fraction z_g is directly sensitive to the parton-shower splitting functions, thereby providing a useful handle to improve their modeling in the MC generators.

The angle between the groomed subjets, ΔR_g, is an experimentally powerful observable for extracting the value of the strong coupling in final-state parton radiation (FSR) processes. A value of $\alpha_S(m_Z) = 0.115^{+0.015}_{-0.013}$, including experimental as well as model uncertainties, has been extracted at leading-order plus leading-log accuracy, where the precision is limited by the FSR scale uncertainty of the PYTHIA 8 prediction. The data will allow for a precise determination of $\alpha_S(m_Z)$ once predictions for top quark decays with multiple emissions at higher order combined with parton showers (ideally at approximate next-leading-log accuracy) are available. Besides tuning and improving final-state parton showers, the present data also provide useful tests for improved quantum chromodynamics analytical calculations, including higher-order fixed and logarithmic corrections, for infrared- and/or collinear-safe observables.

References

[1] A. Buckley et al., "General-purpose event generators for LHC physics", *Phys. Rep.* **504** (2011) 145, `doi:10.1016/j.physrep.2011.03.005`, `arXiv:1101.2599`.

[2] CDF Collaboration, "Study of jet shapes in inclusive jet production in $p\overline{p}$ collisions at $\sqrt{s} = 1.96$ TeV", *Phys. Rev. D* **71** (2005) 112002, `doi:10.1103/PhysRevD.71.112002`, `arXiv:hep-ex/0505013`.

[3] CDF Collaboration, "Measurement of b jet shapes in inclusive jet production in $p\overline{p}$ collisions at $\sqrt{s} = 1.96$ TeV", *Phys. Rev. D* **78** (2008) 072005, `doi:10.1103/PhysRevD.78.072005`, `arXiv:0806.1699`.

[4] CDF Collaboration, "Study of substructure of high transverse momentum jets produced in proton-antiproton collisions at $\sqrt{s} = 1.96$ TeV", *Phys. Rev. D* **85** (2012) 091101, `doi:10.1103/PhysRevD.85.091101`, `arXiv:1106.5952`.

[5] ZEUS Collaboration, "Measurement of subjet multiplicities in neutral current deep inelastic scattering at HERA and determination of α_S", *Phys. Lett. B* **558** (2003) 41, `doi:10.1016/S0370-2693(03)00216-8`, `arXiv:hep-ex/0212030`.

[6] ZEUS Collaboration, "Substructure dependence of jet cross sections at HERA and determination of α_S", *Nucl. Phys. B* **700** (2004) 3, `doi:10.1016/j.nuclphysb.2004.08.049`, `arXiv:hep-ex/0405065`.

[7] ZEUS Collaboration, "Subjet distributions in deep inelastic scattering at HERA", *Eur. Phys. J. C* **63** (2009) 527, `doi:10.1140/epjc/s10052-009-1090-3`, `arXiv:0812.2864`.

[8] ALEPH Collaboration, "Studies of QCD at e^+e^- centre-of-mass energies between 91 GeV and 209 GeV", *Eur. Phys. J. C* **35** (2004) 457, `doi:10.1140/epjc/s2004-01891-4`.

[9] DELPHI Collaboration, "Tuning and test of fragmentation models based on identified particles and precision event shape data", *Z. Phys. C* **73** (1996) 11, `doi:10.1007/s002880050295`.

[10] DELPHI Collaboration, "A study of the b-quark fragmentation function with the
DELPHI detector at LEP I and an averaged distribution obtained at the Z pole", *Eur.
Phys. J. C* **71** (2011) 1557, `doi:10.1140/epjc/s10052-011-1557-x`,
`arXiv:1102.4748`.

[11] L3 Collaboration, "Studies of hadronic event structure in e^+e^- annihilation from $30\,\mathrm{GeV}$
to $209\,\mathrm{GeV}$ with the L3 detector", *Phys. Rep.* **399** (2004) 71,
`doi:10.1016/j.physrep.2004.07.002`, `arXiv:hep-ex/0406049`.

[12] OPAL Collaboration, "Measurement of event shape distributions and moments in e^+e^-
$\rightarrow$ hadrons at $91\,\mathrm{GeV}$- $209\,\mathrm{GeV}$ and a determination of α_s", *Eur. Phys. J. C* **40** (2005) 287,
`doi:10.1140/epjc/s2005-02120-6`, `arXiv:hep-ex/0503051`.

[13] OPAL Collaboration, "Measurements of flavor dependent fragmentation functions in
$Z^0 \rightarrow q\bar{q}$ events", *Eur. Phys. J. C* **7** (1999) 369, `doi:10.1007/s100529901067`,
`arXiv:hep-ex/9807004`.

[14] SLD Collaboration, "Production of $\pi^+, K^+, K^0, K^{*0}, \phi, p$ and Λ^0 in hadronic Z^0 decays",
Phys. Rev. D **59** (1999) 052001, `doi:10.1103/PhysRevD.59.052001`,
`arXiv:hep-ex/9805029`.

[15] SLD Collaboration, "Measurement of the b quark fragmentation function in Z^0 decays",
Phys. Rev. D **65** (2002) 092006, `doi:10.1103/PhysRevD.65.092006`,
`arXiv:hep-ex/0202031`. [Erratum: `doi:10.1103/PhysRevD.66.079905`].

[16] S. D. Ellis, C. K. Vermilion, and J. R. Walsh, "Techniques for improved heavy particle
searches with jet substructure", *Phys. Rev. D* **80** (2009) 051501,
`doi:10.1103/PhysRevD.80.051501`, `arXiv:0903.5081`.

[17] A. Altheimer et al., "Boosted objects and jet substructure at the LHC. Report of
BOOST2012, held at IFIC Valencia, 23rd-27th of July 2012", *Eur. Phys. J. C* **74** (2014)
2792, `doi:10.1140/epjc/s10052-014-2792-8`, `arXiv:1311.2708`.

[18] D. d'Enterria and P. Z. Skands, eds., "Parton radiation and fragmentation from LHC to
FCC-ee". (2017). `arXiv:1702.01329`.

[19] A. J. Larkoski, I. Moult, and B. Nachman, "Jet substructure at the Large Hadron
Collider: a review of recent advances in theory and machine learning", (2017).
`arXiv:1709.04464`.

[20] S. Marzani, L. Schunk, and G. Soyez, "A study of jet mass distributions with grooming",
JHEP **07** (2017) 132, `doi:10.1007/JHEP07(2017)132`, `arXiv:1704.02210`.

[21] C. Frye, A. J. Larkoski, M. D. Schwartz, and K. Yan, "Factorization for groomed jet
substructure beyond the next-to-leading logarithm", *JHEP* **07** (2016) 064,
`doi:10.1007/JHEP07(2016)064`, `arXiv:1603.09338`.

[22] ATLAS Collaboration, "Study of jet shapes in inclusive jet production in pp collisions at
$\sqrt{s} = 7$ TeV using the ATLAS detector", *Phys. Rev. D* **83** (2011) 052003,
`doi:10.1103/PhysRevD.83.052003`, `arXiv:1101.0070`.

[23] ATLAS Collaboration, "ATLAS measurements of the properties of jets for boosted
particle searches", *Phys. Rev. D* **86** (2012) 072006,
`doi:10.1103/PhysRevD.86.072006`, `arXiv:1206.5369`.

[24] CMS Collaboration, "Studies of jet mass in dijet and W/Z+jet events", *JHEP* **05** (2013) 090, `doi:10.1007/JHEP05(2013)090`, `arXiv:1303.4811`.

[25] CMS Collaboration, "Measurements of jet charge with dijet events in pp collisions at $\sqrt{s} = 8$ TeV", *JHEP* **10** (2017) 131, `doi:10.1007/JHEP10(2017)131`, `arXiv:1706.05868`.

[26] ATLAS Collaboration, "A measurement of the soft-drop jet mass in pp collisions at $\sqrt{s} = 13$ TeV with the ATLAS detector", 2018.

[27] CMS Collaboration, "Measurements of the differential jet cross section as a function of the jet mass in dijet events from proton-proton collisions at $\sqrt{s} = 13$ TeV", (2018). `arXiv:1807.05974`. Submitted to *JHEP*.

[28] ATLAS Collaboration, "Measurement of jet shapes in top-quark pair events at $\sqrt{s} = 7$ TeV using the ATLAS detector", *Eur. Phys. J. C* **73** (2013) 2676, `doi:10.1140/epjc/s10052-013-2676-3`, `arXiv:1307.5749`.

[29] CMS Collaboration, "Measurement of the jet mass in highly boosted $t\bar{t}$ events from pp collisions at $\sqrt{s} = 8$ TeV", *Eur. Phys. J. C* **77** (2017) 467, `doi:10.1140/epjc/s10052-017-5030-3`, `arXiv:1703.06330`.

[30] CMS Collaboration, "The CMS trigger system", *JINST* **12** (2017) P01020, `doi:10.1088/1748-0221/12/01/P01020`, `arXiv:1609.02366`.

[31] CMS Collaboration, "The CMS experiment at the CERN LHC", *JINST* **3** (2008) S08004, `doi:10.1088/1748-0221/3/08/S08004`.

[32] P. Nason, "A new method for combining NLO QCD with shower Monte Carlo algorithms", *JHEP* **11** (2004) 040, `doi:10.1088/1126-6708/2004/11/040`, `arXiv:hep-ph/0409146`.

[33] S. Frixione, P. Nason, and C. Oleari, "Matching NLO QCD computations with parton shower simulations: the POWHEG method", *JHEP* **11** (2007) 070, `doi:10.1088/1126-6708/2007/11/070`, `arXiv:0709.2092`.

[34] S. Alioli, P. Nason, C. Oleari, and E. Re, "A general framework for implementing NLO calculations in shower Monte Carlo programs: the POWHEG BOX ", *JHEP* **06** (2010) 043, `doi:10.1007/JHEP06(2010)043`, `arXiv:1002.2581`.

[35] S. Frixione, P. Nason, and G. Ridolfi, "A positive-weight next-to-leading-order Monte Carlo for heavy flavour hadroproduction", *JHEP* **09** (2007) 126, `doi:10.1088/1126-6708/2007/09/126`, `arXiv:0707.3088`.

[36] M. Czakon and A. Mitov, "Top++: A program for the calculation of the top-pair cross-section at hadron colliders", *Comput. Phys. Commun.* **185** (2014) 2930, `doi:10.1016/j.cpc.2014.06.021`, `arXiv:1112.5675`.

[37] J. Alwall et al., "The automated computation of tree-level and next-to-leading order differential cross sections, and their matching to parton shower simulations", *JHEP* **07** (2014) 079, `doi:10.1007/JHEP07(2014)079`, `arXiv:1405.0301`.

[38] R. Frederix and S. Frixione, "Merging meets matching in MC@NLO", *JHEP* **12** (2012) 061, `doi:10.1007/JHEP12(2012)061`, `arXiv:1209.6215`.

[39] J. Alwall et al., "Comparative study of various algorithms for the merging of parton showers and matrix elements in hadronic collisions", *Eur. Phys. J. C* **53** (2008) 473, `doi:10.1140/epjc/s10052-007-0490-5`, `arXiv:0706.2569`.

[40] T. Melia, P. Nason, R. Rontsch, and G. Zanderighi, "W^+W^-, WZ and ZZ production in the POWHEG BOX", *JHEP* **11** (2011) 078, `doi:10.1007/JHEP11(2011)078`, `arXiv:1107.5051`.

[41] E. Re, "Single-top Wt-channel production matched with parton showers using the POWHEG method", *Eur. Phys. J. C* **71** (2011) 1547, `doi:10.1140/epjc/s10052-011-1547-z`, `arXiv:1009.2450`.

[42] S. Alioli, P. Nason, C. Oleari, and E. Re, "NLO single-top production matched with shower in POWHEG: *s*- and *t*-channel contributions", *JHEP* **09** (2009) 111, `doi:10.1088/1126-6708/2009/09/111`, `arXiv:0907.4076`. [Erratum: JHEP **02** (2010) 011].

[43] S. Frixione, E. Laenen, P. Motylinski, and B. R. Webber, "Angular correlations of lepton pairs from vector boson and top quark decays in Monte Carlo simulations", *JHEP* **04** (2007) 081, `doi:10.1088/1126-6708/2007/04/081`, `arXiv:hep-ph/0702198`.

[44] P. Artoisenet, R. Frederix, O. Mattelaer, and R. Rietkerk, "Automatic spin-entangled decays of heavy resonances in Monte Carlo simulations", *JHEP* **03** (2013) 015, `doi:10.1007/JHEP03(2013)015`, `arXiv:1212.3460`.

[45] T. Sjöstrand et al., "An introduction to PYTHIA 8.2", *Comput. Phys. Commun.* **191** (2015) 159, `doi:10.1016/j.cpc.2015.01.024`, `arXiv:1410.3012`.

[46] NNPDF Collaboration, "Parton distributions for the LHC Run II", *JHEP* **04** (2015) 040, `doi:10.1007/JHEP04(2015)040`, `arXiv:1410.8849`.

[47] E. Norrbin and T. Sjöstrand, "QCD radiation off heavy particles", *Nucl. Phys. B* **603** (2001) 297, `doi:10.1016/S0550-3213(01)00099-2`, `arXiv:hep-ph/0010012`.

[48] B. Andersson, G. Gustafson, G. Ingelman, and T. Sjöstrand, "Parton fragmentation and string dynamics", *Phys. Rep.* **97** (1983) 31, `doi:10.1016/0370-1573(83)90080-7`.

[49] T. Sjöstrand, "Jet fragmentation of nearby partons", *Nucl. Phys. B* **248** (1984) 469, `doi:10.1016/0550-3213(84)90607-2`.

[50] M. G. Bowler, "e^+e^- production of heavy quarks in the string model", *Z. Phys. C* **11** (1981) 169, `doi:10.1007/BF01574001`.

[51] CMS Collaboration, "Investigations of the impact of the parton shower tuning in PYTHIA 8 in the modelling of $t\bar{t}$ at $\sqrt{s} = 8$ and 13 TeV", Technical Report CMS-PAS-TOP-16-021, 2016.

[52] CMS Collaboration, "Event generator tunes obtained from underlying event and multiparton scattering measurements", *Eur. Phys. J. C* **76** (2016) 155, `doi:10.1140/epjc/s10052-016-3988-x`, `arXiv:1512.00815`.

[53] M. Bähr et al., "HERWIG++ physics and manual", *Eur. Phys. J. C* **58** (2008) 639, `doi:10.1140/epjc/s10052-008-0798-9`, `arXiv:0803.0883`.

[54] S. Gieseke, P. Stephens, and B. Webber, "New formalism for QCD parton showers", *JHEP* **12** (2003) 045, `doi:10.1088/1126-6708/2003/12/045`, `arXiv:hep-ph/0310083`.

[55] B. R. Webber, "A QCD model for jet fragmentation including soft gluon interference", *Nucl. Phys. B* **238** (1984) 492, `doi:10.1016/0550-3213(84)90333-X`.

[56] GEANT4 Collaboration, "GEANT4 — a simulation toolkit", *Nucl. Instrum. Meth. A* **506** (2003) 250, `doi:10.1016/S0168-9002(03)01368-8`.

[57] J. Bellm et al., "HERWIG 7.0/HERWIG ++ 3.0 release note", *Eur. Phys. J. C* **76** (2016) 196, `doi:10.1140/epjc/s10052-016-4018-8`, `arXiv:1512.01178`.

[58] T. Gleisberg et al., "Event generation with SHERPA 1.1", *JHEP* **02** (2009) 007, `doi:10.1088/1126-6708/2009/02/007`, `arXiv:0811.4622`.

[59] S. Frixione and B. R. Webber, "Matching NLO QCD computations and parton shower simulations", *JHEP* **06** (2002) 029, `doi:10.1088/1126-6708/2002/06/029`, `arXiv:hep-ph/0204244`.

[60] S. Schumann and F. Krauss, "A parton shower algorithm based on Catani-Seymour dipole factorisation", *JHEP* **03** (2008) 038, `doi:10.1088/1126-6708/2008/03/038`, `arXiv:0709.1027`.

[61] J.-C. Winter, F. Krauss, and G. Soff, "A modified cluster hadronization model", *Eur. Phys. J. C* **36** (2004) 381, `doi:10.1140/epjc/s2004-01960-8`, `arXiv:hep-ph/0311085`.

[62] S. Catani, B. R. Webber, and G. Marchesini, "QCD coherent branching and semiinclusive processes at large x", *Nucl. Phys. B* **349** (1991) 635, `doi:10.1016/0550-3213(91)90390-J`.

[63] S. Höche and S. Prestel, "The midpoint between dipole and parton showers", *Eur. Phys. J. C* **75** (2015) 461, `doi:10.1140/epjc/s10052-015-3684-2`, `arXiv:1506.05057`.

[64] S. Höche and S. Prestel, "Triple collinear emissions in parton showers", *Phys. Rev. D* **96** (2017) 074017, `doi:10.1103/PhysRevD.96.074017`, `arXiv:1705.00742`.

[65] S. Höche, F. Krauss, and S. Prestel, "Implementing NLO DGLAP evolution in parton showers", *JHEP* **10** (2017) 093, `doi:10.1007/JHEP10(2017)093`, `arXiv:1705.00982`.

[66] T. Sjöstrand and M. van Zijl, "A multiple interaction model for the event structure in hadron collisions", *Phys. Rev. D* **36** (1987) 2019, `doi:10.1103/PhysRevD.36.2019`.

[67] J. M. Butterworth, J. R. Forshaw, and M. H. Seymour, "Multiparton interactions in photoproduction at HERA", *Z. Phys. C* **72** (1996) 637, `doi:10.1007/s002880050286`, `arXiv:hep-ph/9601371`.

[68] I. Borozan and M. H. Seymour, "An eikonal model for multiparticle production in hadron hadron interactions", *JHEP* **09** (2002) 015, `doi:10.1088/1126-6708/2002/09/015`, `arXiv:hep-ph/0207283`.

[69] M. Bahr, S. Gieseke, and M. H. Seymour, "Simulation of multiple partonic interactions in HERWIG ++", *JHEP* **07** (2008) 076, `doi:10.1088/1126-6708/2008/07/076`, `arXiv:0803.3633`.

[70] S. Gieseke, C. Rohr, and A. Siodmok, "Colour reconnections in HERWIG ++", *Eur. Phys. J. C* **72** (2012) 2225, `doi:10.1140/epjc/s10052-012-2225-5`, `arXiv:1206.0041`.

[71] CMS Collaboration, "Particle-flow reconstruction and global event description with the CMS detector", *JINST* **12** (2017) P10003, `doi:10.1088/1748-0221/12/10/P10003`, `arXiv:1706.04965`.

[72] M. Cacciari, G. P. Salam, and G. Soyez, "The anti-k_t jet clustering algorithm", *JHEP* **04** (2008) 063, `doi:10.1088/1126-6708/2008/04/063`, `arXiv:0802.1189`.

[73] M. Cacciari, G. P. Salam, and G. Soyez, "FastJet user manual", *Eur. Phys. J. C* **72** (2012) 1896, `doi:10.1140/epjc/s10052-012-1896-2`, `arXiv:1111.6097`.

[74] CMS Collaboration, "Jet energy scale and resolution in the CMS experiment in pp collisions at 8 TeV", *JINST* **12** (2017) P02014, `doi:10.1088/1748-0221/12/02/P02014`, `arXiv:1607.03663`.

[75] CMS Collaboration, "Performance of electron reconstruction and selection with the CMS detector in proton-proton collisions at $\sqrt{s} = 8\,$TeV", *JINST* **10** (2015) P06005, `doi:10.1088/1748-0221/10/06/P06005`, `arXiv:1502.02701`.

[76] CMS Collaboration, "Performance of the CMS muon detector and muon reconstruction with proton-proton collisions at $\sqrt{s} = 13\,$TeV", *JINST* **13** (2018) P06015, `doi:10.1088/1748-0221/13/06/P06015`, `arXiv:1804.04528`.

[77] CMS Collaboration, "Identification of b-quark jets with the CMS experiment", *JINST* **8** (2013) P04013, `doi:10.1088/1748-0221/8/04/P04013`, `arXiv:1211.4462`.

[78] CMS Collaboration, "Identification of heavy-flavour jets with the CMS detector in pp collisions at 13 TeV", *JINST* **13** (2018) P05011, `doi:10.1088/1748-0221/13/05/P05011`, `arXiv:1712.07158`.

[79] CMS Collaboration, "Object definitions for top quark analyses at the particle level", Technical Report CMS-NOTE-2017-004, 2017.

[80] M. Cacciari, G. P. Salam, and G. Soyez, "The catchment area of jets", *JHEP* **04** (2008) 005, `doi:10.1088/1126-6708/2008/04/005`, `arXiv:0802.1188`.

[81] S. Schmitt, "TUnfold: an algorithm for correcting migration effects in high energy physics", *JINST* **7** (2012) T10003, `doi:10.1088/1748-0221/7/10/T10003`, `arXiv:1205.6201`.

[82] CMS Collaboration, "Measurement of the inelastic proton-proton cross section at $\sqrt{s} = 13\,$TeV", *JHEP* **07** (2018) 161, `doi:10.1007/JHEP07(2018)161`, `arXiv:1802.02613`.

[83] M. Aliev et al., "HATHOR: HAdronic Top and Heavy quarks crOss section calculatoR", *Comput. Phys. Commun.* **182** (2011) 1034, `doi:10.1016/j.cpc.2010.12.040`, `arXiv:1007.1327`.

[84] P. Kant et al., "HatHor for single top-quark production: Updated predictions and uncertainty estimates for single top-quark production in hadronic collisions", *Comput. Phys. Commun.* **191** (2015) 74, `doi:10.1016/j.cpc.2015.02.001`, `arXiv:1406.4403`.

[85] N. Kidonakis, "Two-loop soft anomalous dimensions for single top quark associated production with a W- or H-", *Phys. Rev. D* **82** (2010) 054018, `doi:10.1103/PhysRevD.82.054018`, `arXiv:1005.4451`.

[86] N. Kidonakis, "Top quark production", in *Proceedings, Helmholtz International Summer School on Physics of Heavy Quarks and Hadrons (HQ 2013): JINR, Dubna, Russia, July 15-28, 2013*, p. 139. 2014. `arXiv:1311.0283`. `doi:10.3204/DESY-PROC-2013-03/Kidonakis`.

[87] S. Dulat et al., "New parton distribution functions from a global analysis of quantum chromodynamics", *Phys. Rev. D* **93** (2016) 033006, `doi:10.1103/PhysRevD.93.033006`, `arXiv:1506.07443`.

[88] L. A. Harland-Lang, A. D. Martin, P. Motylinski, and R. S. Thorne, "Parton distributions in the LHC era: MMHT 2014 PDFs", *Eur. Phys. J. C* **75** (2015) 204, `doi:10.1140/epjc/s10052-015-3397-6`, `arXiv:1412.3989`.

[89] J. R. Christiansen and P. Z. Skands, "String formation beyond leading colour", *JHEP* **08** (2015) 003, `doi:10.1007/JHEP08(2015)003`, `arXiv:1505.01681`.

[90] S. Argyropoulos and T. Sjöstrand, "Effects of color reconnection on $t\bar{t}$ final states at the LHC", *JHEP* **11** (2014) 043, `doi:10.1007/JHEP11(2014)043`, `arXiv:1407.6653`.

[91] ALEPH Collaboration, "Study of the fragmentation of b quarks into B mesons at the Z peak", *Phys. Lett. B* **512** (2001) 30, `doi:10.1016/S0370-2693(01)00690-6`, `arXiv:hep-ex/0106051`.

[92] OPAL Collaboration, "Inclusive analysis of the b quark fragmentation function in Z decays at LEP", *Eur. Phys. J. C* **29** (2003) 463, `doi:10.1140/epjc/s2003-01229-x`, `arXiv:hep-ex/0210031`.

[93] C. Peterson, D. Schlatter, I. Schmitt, and P. M. Zerwas, "Scaling violations in inclusive e^+e^- annihilation spectra", *Phys. Rev. D* **27** (1983) 105, `doi:10.1103/PhysRevD.27.105`.

[94] Particle Data Group Collaboration, "Review of particle physics", *Chin. Phys. C* **40** (2016) 100001, `doi:10.1088/1674-1137/40/10/100001`.

[95] CMS Collaboration, "Measurement of the top quark mass using proton-proton data at $\sqrt{s}$ = 7 and 8 TeV", *Phys. Rev. D* **93** (2016) 072004, `doi:10.1103/PhysRevD.93.072004`, `arXiv:1509.04044`.

[96] CMS Collaboration, "Measurement of differential cross sections for top quark pair production using the lepton+jets final state in proton-proton collisions at 13 TeV", *Phys. Rev. D* **95** (2017) 092001, `doi:10.1103/PhysRevD.95.092001`, `arXiv:1610.04191`.

[97] CMS Collaboration, "Measurement of normalized differential $t\bar{t}$ cross sections in the dilepton channel from pp collisions at $\sqrt{s}$ = 13 TeV", *JHEP* **04** (2018) 060, `doi:10.1007/JHEP04(2018)060`, `arXiv:1708.07638`.

[98] CMS Collaboration, "Description and performance of track and primary-vertex reconstruction with the CMS tracker", *JINST* **9** (2014) P10009, `doi:10.1088/1748-0221/9/10/P10009`, `arXiv:1405.6569`.

[99] A. Buckley and M. Whalley, "HepData reloaded: reinventing the HEP data archive", in *Proceedings, 13th International Workshop on Advanced computing and analysis techniques in physics research (ACAT2010)*, p. 067. Jaipur, India, February, 2010. `arXiv:1006.0517`. [PoS(ACAT2010)067]. `doi:10.22323/1.093.0067`.

[100] E. Maguire, L. Heinrich, and G. Watt, "HEPData: a repository for high energy physics data", *J. Phys. Conf. Ser.* **898** (2017) 102006, `doi:10.1088/1742-6596/898/10/102006`, `arXiv:1704.05473`.

[101] A. J. Larkoski, J. Thaler, and W. J. Waalewijn, "Gaining (mutual) information about quark/gluon discrimination", *JHEP* **11** (2014) 129, `doi:10.1007/JHEP11(2014)129`, `arXiv:1408.3122`.

[102] D. Bertolini, T. Chan, and J. Thaler, "Jet observables without jet algorithms", *JHEP* **04** (2014) 013, `doi:10.1007/JHEP04(2014)013`, `arXiv:1310.7584`.

[103] A. J. Larkoski, D. Neill, and J. Thaler, "Jet shapes with the broadening axis", *JHEP* **04** (2014) 017, `doi:10.1007/JHEP04(2014)017`, `arXiv:1401.2158`.

[104] A. J. Larkoski, S. Marzani, and J. Thaler, "Sudakov safety in perturbative QCD", *Phys. Rev. D* **91** (2015) 111501, `doi:10.1103/PhysRevD.91.111501`, `arXiv:1502.01719`.

[105] ATLAS Collaboration, "ATLAS run 1 PYTHIA 8 tunes", Technical Report ATL-PHYS-PUB-2014-021, 2014.

[106] ATLAS Collaboration, "Measurement of the charged-particle multiplicity inside jets from $\sqrt{s} = 8$ TeV pp collisions with the ATLAS detector", *Eur. Phys. J. C* **76** (2016) 322, `doi:10.1140/epjc/s10052-016-4126-5`, `arXiv:1602.00988`.

[107] CMS Collaboration, "Search for a Higgs boson in the decay channel $H \to ZZ^{(*)} \to q\bar{q}\ell^-\ell^+$ in pp collisions at $\sqrt{s} = 7$ TeV", *JHEP* **04** (2012) 036, `doi:10.1007/JHEP04(2012)036`, `arXiv:1202.1416`.

[108] J. R. Andersen et al., "Les Houches 2015: Physics at TeV Colliders Standard Model Working Group Report", in *9th Les Houches Workshop on Physics at TeV Colliders (PhysTeV 2015) Les Houches, France, June 1-19, 2015*. `arXiv:1605.04692`.

[109] S. Catani, G. Turnock, and B. Webber, "Jet broadening measures in e^+e^- annihilation", *Phys. Lett. B* **295** (1992) 269, `doi:10.1016/0370-2693(92)91565-Q`.

[110] P. Rakow and B. Webber, "Transverse momentum moments of hadron distributions in QCD jets", *Nucl. Phys. B* **191** (1981) 63, `doi:10.1016/0550-3213(81)90286-8`.

[111] R. K. Ellis and B. R. Webber, "QCD jet broadening in hadron hadron collisions", in *Physics of the Superconducting Supercollider: Proceedings, 1986 Summer Study*, p. 74. American Institue of Physics, June, July, 1986. Conf. Proc. C, 860623.

[112] E. Farhi, "Quantum chromodynamics test for jets", *Phys. Rev. Lett.* **39** (1977) 1587, `doi:10.1103/PhysRevLett.39.1587`.

[113] S. V. Chekanov and J. Proudfoot, "Searches for TeV-scale particles at the LHC using jet shapes", *Phys. Rev. D* **81** (2010) 114038, `doi:10.1103/PhysRevD.81.114038`, `arXiv:1002.3982`.

[114] Y. L. Dokshitzer, G. D. Leder, S. Moretti, and B. R. Webber, "Better jet clustering algorithms", *JHEP* **08** (1997) 001, `doi:10.1088/1126-6708/1997/08/001`, `arXiv:hep-ph/9707323`.

[115] M. Wöbisch and T. Wengler, "Hadronization corrections to jet cross sections in deep-inelastic scattering", (1998). `arXiv:hep-ph/9907280`.

[116] A. J. Larkoski, S. Marzani, G. Soyez, and J. Thaler, "Soft drop", *JHEP* **05** (2014) 146, `doi:10.1007/JHEP05(2014)146`, `arXiv:1402.2657`.

[117] M. Dasgupta, A. Fregoso, S. Marzani, and G. P. Salam, "Towards an understanding of jet substructure", *JHEP* **09** (2013) 029, `doi:10.1007/JHEP09(2013)029`, `arXiv:1307.0007`.

[118] A. Larkoski et al., "Exposing the QCD splitting function with CMS Open Data", *Phys. Rev. Lett.* **119** (2017) 132003, `doi:10.1103/PhysRevLett.119.132003`, `arXiv:1704.05066`.

[119] CMS Collaboration, "Measurement of the splitting function in pp and PbPb collisions at $\sqrt{s_{\mathrm{NN}}} = 5.02$ TeV", *Phys. Rev. Lett.* **120** (2018) 142302, `doi:10.1103/PhysRevLett.120.142302`, `arXiv:1708.09429`.

[120] C. Frye, A. J. Larkoski, J. Thaler, and K. Zhou, "Casimir meets Poisson: improved quark/gluon discrimination with counting observables", *JHEP* **09** (2017) 083, `doi:10.1007/JHEP09(2017)083`, `arXiv:1704.06266`.

[121] S. D. Ellis and D. E. Soper, "Successive combination jet algorithm for hadron collisions", *Phys. Rev. D* **48** (1993) 3160, `doi:10.1103/PhysRevD.48.3160`, `arXiv:hep-ph/9305266`.

[122] J. Thaler and K. Van Tilburg, "Identifying boosted objects with N-subjettiness", *JHEP* **03** (2011) 015, `doi:10.1007/JHEP03(2011)015`, `arXiv:1011.2268`.

[123] J. Thaler and K. Van Tilburg, "Maximizing boosted top identification by minimizing N-subjettiness", *JHEP* **02** (2012) 093, `doi:10.1007/JHEP02(2012)093`, `arXiv:1108.2701`.

[124] A. J. Larkoski, G. P. Salam, and J. Thaler, "Energy correlation functions for jet substructure", *JHEP* **06** (2013) 108, `doi:10.1007/JHEP06(2013)108`, `arXiv:1305.0007`.

[125] I. Moult, L. Necib, and J. Thaler, "New angles on energy correlation functions", *JHEP* **12** (2016) 153, `doi:10.1007/JHEP12(2016)153`, `arXiv:1609.07483`.

[126] C. Bierlich, G. Gustafson, L. Lönnblad, and A. Tarasov, "Effects of overlapping strings in pp collisions", *JHEP* **03** (2015) 148, `doi:10.1007/JHEP03(2015)148`, `arXiv:1412.6259`.

A   The CMS Collaboration

Yerevan Physics Institute, Yerevan, Armenia
A.M. Sirunyan, A. Tumasyan

Institut für Hochenergiephysik, Wien, Austria
W. Adam, F. Ambrogi, E. Asilar, T. Bergauer, J. Brandstetter, E. Brondolin, M. Dragicevic, J. Erö, A. Escalante Del Valle, M. Flechl, R. Frühwirth[1], V.M. Ghete, J. Hrubec, M. Jeitler[1], N. Krammer, I. Krätschmer, D. Liko, T. Madlener, I. Mikulec, N. Rad, H. Rohringer, J. Schieck[1], R. Schöfbeck, M. Spanring, D. Spitzbart, A. Taurok, W. Waltenberger, J. Wittmann, C.-E. Wulz[1], M. Zarucki

Institute for Nuclear Problems, Minsk, Belarus
V. Chekhovsky, V. Mossolov, J. Suarez Gonzalez

Universiteit Antwerpen, Antwerpen, Belgium
E.A. De Wolf, D. Di Croce, X. Janssen, J. Lauwers, M. Pieters, M. Van De Klundert, H. Van Haevermaet, P. Van Mechelen, N. Van Remortel

Vrije Universiteit Brussel, Brussel, Belgium
S. Abu Zeid, F. Blekman, J. D'Hondt, I. De Bruyn, J. De Clercq, K. Deroover, G. Flouris, D. Lontkovskyi, S. Lowette, I. Marchesini, S. Moortgat, L. Moreels, Q. Python, K. Skovpen, S. Tavernier, W. Van Doninck, P. Van Mulders, I. Van Parijs

Université Libre de Bruxelles, Bruxelles, Belgium
D. Beghin, B. Bilin, H. Brun, B. Clerbaux, G. De Lentdecker, H. Delannoy, B. Dorney, G. Fasanella, L. Favart, R. Goldouzian, A. Grebenyuk, A.K. Kalsi, T. Lenzi, J. Luetic, N. Postiau, E. Starling, L. Thomas, C. Vander Velde, P. Vanlaer, D. Vannerom, Q. Wang

Ghent University, Ghent, Belgium
T. Cornelis, D. Dobur, A. Fagot, M. Gul, I. Khvastunov[2], D. Poyraz, C. Roskas, D. Trocino, M. Tytgat, W. Verbeke, B. Vermassen, M. Vit, N. Zaganidis

Université Catholique de Louvain, Louvain-la-Neuve, Belgium
H. Bakhshiansohi, O. Bondu, S. Brochet, G. Bruno, C. Caputo, P. David, C. Delaere, M. Delcourt, B. Francois, A. Giammanco, G. Krintiras, V. Lemaitre, A. Magitteri, A. Mertens, M. Musich, K. Piotrzkowski, A. Saggio, M. Vidal Marono, S. Wertz, J. Zobec

Centro Brasileiro de Pesquisas Fisicas, Rio de Janeiro, Brazil
F.L. Alves, G.A. Alves, L. Brito, G. Correia Silva, C. Hensel, A. Moraes, M.E. Pol, P. Rebello Teles

Universidade do Estado do Rio de Janeiro, Rio de Janeiro, Brazil
E. Belchior Batista Das Chagas, W. Carvalho, J. Chinellato[3], E. Coelho, E.M. Da Costa, G.G. Da Silveira[4], D. De Jesus Damiao, C. De Oliveira Martins, S. Fonseca De Souza, H. Malbouisson, D. Matos Figueiredo, M. Melo De Almeida, C. Mora Herrera, L. Mundim, H. Nogima, W.L. Prado Da Silva, L.J. Sanchez Rosas, A. Santoro, A. Sznajder, M. Thiel, E.J. Tonelli Manganote[3], F. Torres Da Silva De Araujo, A. Vilela Pereira

Universidade Estadual Paulista ^{a}, Universidade Federal do ABC ^{b}, São Paulo, Brazil
S. Ahuja[a], C.A. Bernardes[a], L. Calligaris[a], T.R. Fernandez Perez Tomei[a], E.M. Gregores[b], P.G. Mercadante[b], S.F. Novaes[a], SandraS. Padula[a], D. Romero Abad[b]

Institute for Nuclear Research and Nuclear Energy, Bulgarian Academy of Sciences, Sofia, Bulgaria
A. Aleksandrov, R. Hadjiiska, P. Iaydjiev, A. Marinov, M. Misheva, M. Rodozov, M. Shopova, G. Sultanov

University of Sofia, Sofia, Bulgaria
A. Dimitrov, L. Litov, B. Pavlov, P. Petkov

Beihang University, Beijing, China
W. Fang[5], X. Gao[5], L. Yuan

Institute of High Energy Physics, Beijing, China
M. Ahmad, J.G. Bian, G.M. Chen, H.S. Chen, M. Chen, Y. Chen, C.H. Jiang, D. Leggat, H. Liao, Z. Liu, F. Romeo, S.M. Shaheen, A. Spiezia, J. Tao, C. Wang, Z. Wang, E. Yazgan, H. Zhang, J. Zhao

State Key Laboratory of Nuclear Physics and Technology, Peking University, Beijing, China
Y. Ban, G. Chen, A. Levin, J. Li, L. Li, Q. Li, Y. Mao, S.J. Qian, D. Wang, Z. Xu

Tsinghua University, Beijing, China
Y. Wang

Universidad de Los Andes, Bogota, Colombia
C. Avila, A. Cabrera, C.A. Carrillo Montoya, L.F. Chaparro Sierra, C. Florez, C.F. González Hernández, M.A. Segura Delgado

University of Split, Faculty of Electrical Engineering, Mechanical Engineering and Naval Architecture, Split, Croatia
B. Courbon, N. Godinovic, D. Lelas, I. Puljak, T. Sculac

University of Split, Faculty of Science, Split, Croatia
Z. Antunovic, M. Kovac

Institute Rudjer Boskovic, Zagreb, Croatia
V. Brigljevic, D. Ferencek, K. Kadija, B. Mesic, A. Starodumov[6], T. Susa

University of Cyprus, Nicosia, Cyprus
M.W. Ather, A. Attikis, M. Kolosova, G. Mavromanolakis, J. Mousa, C. Nicolaou, F. Ptochos, P.A. Razis, H. Rykaczewski

Charles University, Prague, Czech Republic
M. Finger[7], M. Finger Jr.[7]

Escuela Politecnica Nacional, Quito, Ecuador
E. Ayala

Universidad San Francisco de Quito, Quito, Ecuador
E. Carrera Jarrin

Academy of Scientific Research and Technology of the Arab Republic of Egypt, Egyptian Network of High Energy Physics, Cairo, Egypt
H. Abdalla[8], A.A. Abdelalim[9,10], A. Mohamed[10]

National Institute of Chemical Physics and Biophysics, Tallinn, Estonia
S. Bhowmik, A. Carvalho Antunes De Oliveira, R.K. Dewanjee, K. Ehataht, M. Kadastik, M. Raidal, C. Veelken

Department of Physics, University of Helsinki, Helsinki, Finland
P. Eerola, H. Kirschenmann, J. Pekkanen, M. Voutilainen

Helsinki Institute of Physics, Helsinki, Finland
J. Havukainen, J.K. Heikkilä, T. Järvinen, V. Karimäki, R. Kinnunen, T. Lampén, K. Lassila-Perini, S. Laurila, S. Lehti, T. Lindén, P. Luukka, T. Mäenpää, H. Siikonen, E. Tuominen, J. Tuominiemi

Lappeenranta University of Technology, Lappeenranta, Finland
T. Tuuva

IRFU, CEA, Université Paris-Saclay, Gif-sur-Yvette, France
M. Besancon, F. Couderc, M. Dejardin, D. Denegri, J.L. Faure, F. Ferri, S. Ganjour, A. Givernaud, P. Gras, G. Hamel de Monchenault, P. Jarry, C. Leloup, E. Locci, J. Malcles, G. Negro, J. Rander, A. Rosowsky, M.Ö. Sahin, M. Titov

Laboratoire Leprince-Ringuet, Ecole polytechnique, CNRS/IN2P3, Université Paris-Saclay, Palaiseau, France
A. Abdulsalam[11], C. Amendola, I. Antropov, F. Beaudette, P. Busson, C. Charlot, R. Granier de Cassagnac, I. Kucher, S. Lisniak, A. Lobanov, J. Martin Blanco, M. Nguyen, C. Ochando, G. Ortona, P. Paganini, P. Pigard, R. Salerno, J.B. Sauvan, Y. Sirois, A.G. Stahl Leiton, A. Zabi, A. Zghiche

Université de Strasbourg, CNRS, IPHC UMR 7178, Strasbourg, France
J.-L. Agram[12], J. Andrea, D. Bloch, J.-M. Brom, E.C. Chabert, V. Cherepanov, C. Collard, E. Conte[12], J.-C. Fontaine[12], D. Gelé, U. Goerlach, M. Jansová, A.-C. Le Bihan, N. Tonon, P. Van Hove

Centre de Calcul de l'Institut National de Physique Nucleaire et de Physique des Particules, CNRS/IN2P3, Villeurbanne, France
S. Gadrat

Université de Lyon, Université Claude Bernard Lyon 1, CNRS-IN2P3, Institut de Physique Nucléaire de Lyon, Villeurbanne, France
S. Beauceron, C. Bernet, G. Boudoul, N. Chanon, R. Chierici, D. Contardo, P. Depasse, H. El Mamouni, J. Fay, L. Finco, S. Gascon, M. Gouzevitch, G. Grenier, B. Ille, F. Lagarde, I.B. Laktineh, H. Lattaud, M. Lethuillier, L. Mirabito, A.L. Pequegnot, S. Perries, A. Popov[13], V. Sordini, M. Vander Donckt, S. Viret, S. Zhang

Georgian Technical University, Tbilisi, Georgia
T. Toriashvili[14]

Tbilisi State University, Tbilisi, Georgia
D. Lomidze

RWTH Aachen University, I. Physikalisches Institut, Aachen, Germany
C. Autermann, L. Feld, M.K. Kiesel, K. Klein, M. Lipinski, M. Preuten, M.P. Rauch, C. Schomakers, J. Schulz, M. Teroerde, B. Wittmer, V. Zhukov[13]

RWTH Aachen University, III. Physikalisches Institut A, Aachen, Germany
A. Albert, D. Duchardt, M. Endres, M. Erdmann, T. Esch, R. Fischer, S. Ghosh, A. Güth, T. Hebbeker, C. Heidemann, K. Hoepfner, H. Keller, S. Knutzen, L. Mastrolorenzo, M. Merschmeyer, A. Meyer, P. Millet, S. Mukherjee, T. Pook, M. Radziej, H. Reithler, M. Rieger, F. Scheuch, A. Schmidt, D. Teyssier

RWTH Aachen University, III. Physikalisches Institut B, Aachen, Germany
G. Flügge, O. Hlushchenko, B. Kargoll, T. Kress, A. Künsken, T. Müller, A. Nehrkorn, A. Nowack, C. Pistone, O. Pooth, H. Sert, A. Stahl[15]

Deutsches Elektronen-Synchrotron, Hamburg, Germany
M. Aldaya Martin, T. Arndt, C. Asawatangtrakuldee, I. Babounikau, K. Beernaert, O. Behnke, U. Behrens, A. Bermúdez Martínez, D. Bertsche, A.A. Bin Anuar, K. Borras[16], V. Botta, A. Campbell, P. Connor, C. Contreras-Campana, F. Costanza, V. Danilov, A. De Wit, M.M. Defranchis, C. Diez Pardos, D. Domínguez Damiani, G. Eckerlin, T. Eichhorn, A. Elwood, E. Eren, E. Gallo[17], A. Geiser, J.M. Grados Luyando, A. Grohsjean, P. Gunnellini, M. Guthoff, M. Haranko, A. Harb, J. Hauk, H. Jung, M. Kasemann, J. Keaveney, C. Kleinwort, J. Knolle, D. Krücker, W. Lange, A. Lelek, T. Lenz, K. Lipka, W. Lohmann[18], R. Mankel, I.-A. Melzer-Pellmann, A.B. Meyer, M. Meyer, M. Missiroli, G. Mittag, J. Mnich, V. Myronenko, S.K. Pflitsch, D. Pitzl, A. Raspereza, M. Savitskyi, P. Saxena, P. Schütze, C. Schwanenberger, R. Shevchenko, A. Singh, N. Stefaniuk, H. Tholen, O. Turkot, A. Vagnerini, G.P. Van Onsem, R. Walsh, Y. Wen, K. Wichmann, C. Wissing, O. Zenaiev

University of Hamburg, Hamburg, Germany
R. Aggleton, S. Bein, L. Benato, A. Benecke, V. Blobel, M. Centis Vignali, T. Dreyer, E. Garutti, D. Gonzalez, J. Haller, A. Hinzmann, A. Karavdina, G. Kasieczka, R. Klanner, R. Kogler, N. Kovalchuk, S. Kurz, V. Kutzner, J. Lange, D. Marconi, J. Multhaup, M. Niedziela, D. Nowatschin, A. Perieanu, A. Reimers, O. Rieger, C. Scharf, P. Schleper, S. Schumann, J. Schwandt, J. Sonneveld, H. Stadie, G. Steinbrück, F.M. Stober, M. Stöver, D. Troendle, A. Vanhoefer, B. Vormwald

Karlsruher Institut fuer Technologie, Karlsruhe, Germany
M. Akbiyik, C. Barth, M. Baselga, S. Baur, E. Butz, R. Caspart, T. Chwalek, F. Colombo, W. De Boer, A. Dierlamm, N. Faltermann, B. Freund, M. Giffels, M.A. Harrendorf, F. Hartmann[15], S.M. Heindl, U. Husemann, F. Kassel[15], I. Katkov[13], S. Kudella, H. Mildner, S. Mitra, M.U. Mozer, Th. Müller, M. Plagge, G. Quast, K. Rabbertz, M. Schröder, I. Shvetsov, G. Sieber, H.J. Simonis, R. Ulrich, S. Wayand, M. Weber, T. Weiler, S. Williamson, C. Wöhrmann, R. Wolf

Institute of Nuclear and Particle Physics (INPP), NCSR Demokritos, Aghia Paraskevi, Greece
G. Anagnostou, G. Daskalakis, T. Geralis, A. Kyriakis, D. Loukas, G. Paspalaki, I. Topsis-Giotis

National and Kapodistrian University of Athens, Athens, Greece
G. Karathanasis, S. Kesisoglou, P. Kontaxakis, A. Panagiotou, N. Saoulidou, E. Tziaferi, K. Vellidis

National Technical University of Athens, Athens, Greece
K. Kousouris, I. Papakrivopoulos, G. Tsipolitis

University of Ioánnina, Ioánnina, Greece
I. Evangelou, C. Foudas, P. Gianneios, P. Katsoulis, P. Kokkas, S. Mallios, N. Manthos, I. Papadopoulos, E. Paradas, J. Strologas, F.A. Triantis, D. Tsitsonis

MTA-ELTE Lendület CMS Particle and Nuclear Physics Group, Eötvös Loránd University, Budapest, Hungary
M. Bartók[19], M. Csanad, N. Filipovic, P. Major, M.I. Nagy, G. Pasztor, O. Surányi, G.I. Veres

Wigner Research Centre for Physics, Budapest, Hungary
G. Bencze, C. Hajdu, D. Horvath[20], Á. Hunyadi, F. Sikler, T.Á. Vámi, V. Veszpremi, G. Vesztergombi[†]

Institute of Nuclear Research ATOMKI, Debrecen, Hungary
N. Beni, S. Czellar, J. Karancsi[21], A. Makovec, J. Molnar, Z. Szillasi

Institute of Physics, University of Debrecen, Debrecen, Hungary
P. Raics, Z.L. Trocsanyi, B. Ujvari

Indian Institute of Science (IISc), Bangalore, India
S. Choudhury, J.R. Komaragiri, P.C. Tiwari

National Institute of Science Education and Research, HBNI, Bhubaneswar, India
S. Bahinipati[22], C. Kar, P. Mal, K. Mandal, A. Nayak[23], D.K. Sahoo[22], S.K. Swain

Panjab University, Chandigarh, India
S. Bansal, S.B. Beri, V. Bhatnagar, S. Chauhan, R. Chawla, N. Dhingra, R. Gupta, A. Kaur, A. Kaur, M. Kaur, S. Kaur, R. Kumar, P. Kumari, M. Lohan, A. Mehta, K. Sandeep, S. Sharma, J.B. Singh, G. Walia

University of Delhi, Delhi, India
A. Bhardwaj, B.C. Choudhary, R.B. Garg, M. Gola, S. Keshri, Ashok Kumar, S. Malhotra, M. Naimuddin, P. Priyanka, K. Ranjan, Aashaq Shah, R. Sharma

Saha Institute of Nuclear Physics, HBNI, Kolkata, India
R. Bhardwaj[24], M. Bharti, R. Bhattacharya, S. Bhattacharya, U. Bhawandeep[24], D. Bhowmik, S. Dey, S. Dutt[24], S. Dutta, S. Ghosh, K. Mondal, S. Nandan, A. Purohit, P.K. Rout, A. Roy, S. Roy Chowdhury, S. Sarkar, M. Sharan, B. Singh, S. Thakur[24]

Indian Institute of Technology Madras, Madras, India
P.K. Behera

Bhabha Atomic Research Centre, Mumbai, India
R. Chudasama, D. Dutta, V. Jha, V. Kumar, P.K. Netrakanti, L.M. Pant, P. Shukla

Tata Institute of Fundamental Research-A, Mumbai, India
T. Aziz, M.A. Bhat, S. Dugad, G.B. Mohanty, N. Sur, B. Sutar, RavindraKumar Verma

Tata Institute of Fundamental Research-B, Mumbai, India
S. Banerjee, S. Bhattacharya, S. Chatterjee, P. Das, M. Guchait, Sa. Jain, S. Karmakar, S. Kumar, M. Maity[25], G. Majumder, K. Mazumdar, N. Sahoo, T. Sarkar[25]

Indian Institute of Science Education and Research (IISER), Pune, India
S. Chauhan, S. Dube, V. Hegde, A. Kapoor, K. Kothekar, S. Pandey, A. Rane, S. Sharma

Institute for Research in Fundamental Sciences (IPM), Tehran, Iran
S. Chenarani[26], E. Eskandari Tadavani, S.M. Etesami[26], M. Khakzad, M. Mohammadi Najafabadi, M. Naseri, F. Rezaei Hosseinabadi, B. Safarzadeh[27], M. Zeinali

University College Dublin, Dublin, Ireland
M. Felcini, M. Grunewald

INFN Sezione di Bari [a], Università di Bari [b], Politecnico di Bari [c], Bari, Italy
M. Abbrescia[a,b], C. Calabria[a,b], A. Colaleo[a], D. Creanza[a,c], L. Cristella[a,b], N. De Filippis[a,c], M. De Palma[a,b], A. Di Florio[a,b], F. Errico[a,b], L. Fiore[a], A. Gelmi[a,b], G. Iaselli[a,c], S. Lezki[a,b], G. Maggi[a,c], M. Maggi[a], G. Miniello[a,b], S. My[a,b], S. Nuzzo[a,b], A. Pompili[a,b], G. Pugliese[a,c], R. Radogna[a], A. Ranieri[a], G. Selvaggi[a,b], A. Sharma[a], L. Silvestris[a,15], R. Venditti[a], P. Verwilligen[a], G. Zito[a]

INFN Sezione di Bologna [a], Università di Bologna [b], Bologna, Italy
G. Abbiendi[a], C. Battilana[a,b], D. Bonacorsi[a,b], L. Borgonovi[a,b], S. Braibant-Giacomelli[a,b], R. Campanini[a,b], P. Capiluppi[a,b], A. Castro[a,b], F.R. Cavallo[a], S.S. Chhibra[a,b], C. Ciocca[a],

G. Codispoti[a,b], M. Cuffiani[a,b], G.M. Dallavalle[a], F. Fabbri[a], A. Fanfani[a,b], P. Giacomelli[a], C. Grandi[a], L. Guiducci[a,b], F. Iemmi[a,b], S. Marcellini[a], G. Masetti[a], A. Montanari[a], F.L. Navarria[a,b], A. Perrotta[a], F. Primavera[a,b,15], A.M. Rossi[a,b], T. Rovelli[a,b], G.P. Siroli[a,b], N. Tosi[a]

INFN Sezione di Catania [a]**, Università di Catania** [b]**, Catania, Italy**
S. Albergo[a,b], A. Di Mattia[a], R. Potenza[a,b], A. Tricomi[a,b], C. Tuve[a,b]

INFN Sezione di Firenze [a]**, Università di Firenze** [b]**, Firenze, Italy**
G. Barbagli[a], K. Chatterjee[a,b], V. Ciulli[a,b], C. Civinini[a], R. D'Alessandro[a,b], E. Focardi[a,b], G. Latino, P. Lenzi[a,b], M. Meschini[a], S. Paoletti[a], L. Russo[a,28], G. Sguazzoni[a], D. Strom[a], L. Viliani[a]

INFN Laboratori Nazionali di Frascati, Frascati, Italy
L. Benussi, S. Bianco, F. Fabbri, D. Piccolo

INFN Sezione di Genova [a]**, Università di Genova** [b]**, Genova, Italy**
F. Ferro[a], F. Ravera[a,b], E. Robutti[a], S. Tosi[a,b]

INFN Sezione di Milano-Bicocca [a]**, Università di Milano-Bicocca** [b]**, Milano, Italy**
A. Benaglia[a], A. Beschi[b], L. Brianza[a,b], F. Brivio[a,b], V. Ciriolo[a,b,15], S. Di Guida[a,d,15], M.E. Dinardo[a,b], S. Fiorendi[a,b], S. Gennai[a], A. Ghezzi[a,b], P. Govoni[a,b], M. Malberti[a,b], S. Malvezzi[a], A. Massironi[a,b], D. Menasce[a], L. Moroni[a], M. Paganoni[a,b], D. Pedrini[a], S. Ragazzi[a,b], T. Tabarelli de Fatis[a,b]

INFN Sezione di Napoli [a]**, Università di Napoli 'Federico II'** [b]**, Napoli, Italy, Università della Basilicata** [c]**, Potenza, Italy, Università G. Marconi** [d]**, Roma, Italy**
S. Buontempo[a], N. Cavallo[a,c], A. Di Crescenzo[a,b], F. Fabozzi[a,c], F. Fienga[a], G. Galati[a], A.O.M. Iorio[a,b], W.A. Khan[a], L. Lista[a], S. Meola[a,d,15], P. Paolucci[a,15], C. Sciacca[a,b], E. Voevodina[a,b]

INFN Sezione di Padova [a]**, Università di Padova** [b]**, Padova, Italy, Università di Trento** [c]**, Trento, Italy**
P. Azzi[a], N. Bacchetta[a], A. Boletti[a,b], A. Bragagnolo, R. Carlin[a,b], P. Checchia[a], M. Dall'Osso[a,b], P. De Castro Manzano[a], T. Dorigo[a], U. Dosselli[a], F. Gasparini[a,b], U. Gasparini[a,b], F. Gonella[a], A. Gozzelino[a], S. Lacaprara[a], P. Lujan, M. Margoni[a,b], A.T. Meneguzzo[a,b], N. Pozzobon[a,b], P. Ronchese[a,b], R. Rossin[a,b], A. Tiko, E. Torassa[a], M. Zanetti[a,b], P. Zotto[a,b], G. Zumerle[a,b]

INFN Sezione di Pavia [a]**, Università di Pavia** [b]**, Pavia, Italy**
A. Braghieri[a], A. Magnani[a], P. Montagna[a,b], S.P. Ratti[a,b], V. Re[a], M. Ressegotti[a,b], C. Riccardi[a,b], P. Salvini[a], I. Vai[a,b], P. Vitulo[a,b]

INFN Sezione di Perugia [a]**, Università di Perugia** [b]**, Perugia, Italy**
L. Alunni Solestizi[a,b], M. Biasini[a,b], G.M. Bilei[a], C. Cecchi[a,b], D. Ciangottini[a,b], L. Fanò[a,b], P. Lariccia[a,b], E. Manoni[a], G. Mantovani[a,b], V. Mariani[a,b], M. Menichelli[a], A. Rossi[a,b], A. Santocchia[a,b], D. Spiga[a]

INFN Sezione di Pisa [a]**, Università di Pisa** [b]**, Scuola Normale Superiore di Pisa** [c]**, Pisa, Italy**
K. Androsov[a], P. Azzurri[a], G. Bagliesi[a], L. Bianchini[a], T. Boccali[a], L. Borrello, R. Castaldi[a], M.A. Ciocci[a,b], R. Dell'Orso[a], G. Fedi[a], F. Fiori[a,c], L. Giannini[a,c], A. Giassi[a], M.T. Grippo[a], F. Ligabue[a,c], E. Manca[a,c], G. Mandorli[a,c], A. Messineo[a,b], F. Palla[a], A. Rizzi[a,b], P. Spagnolo[a], R. Tenchini[a], G. Tonelli[a,b], A. Venturi[a], P.G. Verdini[a]

INFN Sezione di Roma [a]**, Sapienza Università di Roma** [b]**, Rome, Italy**
L. Barone[a,b], F. Cavallari[a], M. Cipriani[a,b], N. Daci[a], D. Del Re[a,b], E. Di Marco[a,b], M. Diemoz[a],

S. Gelli[a,b], E. Longo[a,b], B. Marzocchi[a,b], P. Meridiani[a], G. Organtini[a,b], F. Pandolfi[a], R. Paramatti[a,b], F. Preiato[a,b], S. Rahatlou[a,b], C. Rovelli[a], F. Santanastasio[a,b]

INFN Sezione di Torino [a], Università di Torino [b], Torino, Italy, Università del Piemonte Orientale [c], Novara, Italy
N. Amapane[a,b], R. Arcidiacono[a,c], S. Argiro[a,b], M. Arneodo[a,c], N. Bartosik[a], R. Bellan[a,b], C. Biino[a], N. Cartiglia[a], F. Cenna[a,b], S. Cometti, M. Costa[a,b], R. Covarelli[a,b], N. Demaria[a], B. Kiani[a,b], C. Mariotti[a], S. Maselli[a], E. Migliore[a,b], V. Monaco[a,b], E. Monteil[a,b], M. Monteno[a], M.M. Obertino[a,b], L. Pacher[a,b], N. Pastrone[a], M. Pelliccioni[a], G.L. Pinna Angioni[a,b], A. Romero[a,b], M. Ruspa[a,c], R. Sacchi[a,b], K. Shchelina[a,b], V. Sola[a], A. Solano[a,b], D. Soldi, A. Staiano[a]

INFN Sezione di Trieste [a], Università di Trieste [b], Trieste, Italy
S. Belforte[a], V. Candelise[a,b], M. Casarsa[a], F. Cossutti[a], G. Della Ricca[a,b], F. Vazzoler[a,b], A. Zanetti[a]

Kyungpook National University, Daegu, Korea
D.H. Kim, G.N. Kim, M.S. Kim, J. Lee, S. Lee, S.W. Lee, C.S. Moon, Y.D. Oh, S. Sekmen, D.C. Son, Y.C. Yang

Chonnam National University, Institute for Universe and Elementary Particles, Kwangju, Korea
H. Kim, D.H. Moon, G. Oh

Hanyang University, Seoul, Korea
J. Goh, T.J. Kim

Korea University, Seoul, Korea
S. Cho, S. Choi, Y. Go, D. Gyun, S. Ha, B. Hong, Y. Jo, K. Lee, K.S. Lee, S. Lee, J. Lim, S.K. Park, Y. Roh

Sejong University, Seoul, Korea
H.S. Kim

Seoul National University, Seoul, Korea
J. Almond, J. Kim, J.S. Kim, H. Lee, K. Lee, K. Nam, S.B. Oh, B.C. Radburn-Smith, S.h. Seo, U.K. Yang, H.D. Yoo, G.B. Yu

University of Seoul, Seoul, Korea
D. Jeon, H. Kim, J.H. Kim, J.S.H. Lee, I.C. Park

Sungkyunkwan University, Suwon, Korea
Y. Choi, C. Hwang, J. Lee, I. Yu

Vilnius University, Vilnius, Lithuania
V. Dudenas, A. Juodagalvis, J. Vaitkus

National Centre for Particle Physics, Universiti Malaya, Kuala Lumpur, Malaysia
I. Ahmed, Z.A. Ibrahim, M.A.B. Md Ali[29], F. Mohamad Idris[30], W.A.T. Wan Abdullah, M.N. Yusli, Z. Zolkapli

Universidad de Sonora (UNISON), Hermosillo, Mexico
A. Castaneda Hernandez[31], J.A. Murillo Quijada

Centro de Investigacion y de Estudios Avanzados del IPN, Mexico City, Mexico
H. Castilla-Valdez, E. De La Cruz-Burelo, M.C. Duran-Osuna, I. Heredia-De La Cruz[32],

R. Lopez-Fernandez, J. Mejia Guisao, R.I. Rabadan-Trejo, G. Ramirez-Sanchez, R Reyes-Almanza, A. Sanchez-Hernandez

Universidad Iberoamericana, Mexico City, Mexico
S. Carrillo Moreno, C. Oropeza Barrera, F. Vazquez Valencia

Benemerita Universidad Autonoma de Puebla, Puebla, Mexico
J. Eysermans, I. Pedraza, H.A. Salazar Ibarguen, C. Uribe Estrada

Universidad Autónoma de San Luis Potosí, San Luis Potosí, Mexico
A. Morelos Pineda

University of Auckland, Auckland, New Zealand
D. Krofcheck

University of Canterbury, Christchurch, New Zealand
S. Bheesette, P.H. Butler

National Centre for Physics, Quaid-I-Azam University, Islamabad, Pakistan
A. Ahmad, M. Ahmad, M.I. Asghar, Q. Hassan, H.R. Hoorani, A. Saddique, M.A. Shah, M. Shoaib, M. Waqas

National Centre for Nuclear Research, Swierk, Poland
H. Bialkowska, M. Bluj, B. Boimska, T. Frueboes, M. Górski, M. Kazana, K. Nawrocki, M. Szleper, P. Traczyk, P. Zalewski

Institute of Experimental Physics, Faculty of Physics, University of Warsaw, Warsaw, Poland
K. Bunkowski, A. Byszuk[33], K. Doroba, A. Kalinowski, M. Konecki, J. Krolikowski, M. Misiura, M. Olszewski, A. Pyskir, M. Walczak

Laboratório de Instrumentação e Física Experimental de Partículas, Lisboa, Portugal
P. Bargassa, C. Beirão Da Cruz E Silva, A. Di Francesco, P. Faccioli, B. Galinhas, M. Gallinaro, J. Hollar, N. Leonardo, L. Lloret Iglesias, M.V. Nemallapudi, J. Seixas, G. Strong, O. Toldaiev, D. Vadruccio, J. Varela

Joint Institute for Nuclear Research, Dubna, Russia
I. Golutvin, I. Gorbunov, V. Karjavin, I. Kashunin, V. Korenkov, G. Kozlov, A. Lanev, A. Malakhov, V. Matveev[34,35], V.V. Mitsyn, P. Moisenz, V. Palichik, V. Perelygin, S. Shmatov, V. Smirnov, V. Trofimov, B.S. Yuldashev[36], A. Zarubin, V. Zhiltsov

Petersburg Nuclear Physics Institute, Gatchina (St. Petersburg), Russia
V. Golovtsov, Y. Ivanov, V. Kim[37], E. Kuznetsova[38], P. Levchenko, V. Murzin, V. Oreshkin, I. Smirnov, D. Sosnov, V. Sulimov, L. Uvarov, S. Vavilov, A. Vorobyev

Institute for Nuclear Research, Moscow, Russia
Yu. Andreev, A. Dermenev, S. Gninenko, N. Golubev, A. Karneyeu, M. Kirsanov, N. Krasnikov, A. Pashenkov, D. Tlisov, A. Toropin

Institute for Theoretical and Experimental Physics, Moscow, Russia
V. Epshteyn, V. Gavrilov, N. Lychkovskaya, V. Popov, I. Pozdnyakov, G. Safronov, A. Spiridonov, A. Stepennov, V. Stolin, M. Toms, E. Vlasov, A. Zhokin

Moscow Institute of Physics and Technology, Moscow, Russia
T. Aushev

National Research Nuclear University 'Moscow Engineering Physics Institute' (MEPhI), Moscow, Russia
M. Chadeeva[39], P. Parygin, D. Philippov, S. Polikarpov[39], E. Popova, V. Rusinov

P.N. Lebedev Physical Institute, Moscow, Russia
V. Andreev, M. Azarkin[35], I. Dremin[35], M. Kirakosyan[35], S.V. Rusakov, A. Terkulov

Skobeltsyn Institute of Nuclear Physics, Lomonosov Moscow State University, Moscow, Russia
A. Baskakov, A. Belyaev, E. Boos, V. Bunichev, M. Dubinin[40], L. Dudko, V. Klyukhin, O. Kodolova, N. Korneeva, I. Lokhtin, I. Miagkov, S. Obraztsov, M. Perfilov, V. Savrin, P. Volkov

Novosibirsk State University (NSU), Novosibirsk, Russia
V. Blinov[41], T. Dimova[41], L. Kardapoltsev[41], D. Shtol[41], Y. Skovpen[41]

Institute for High Energy Physics of National Research Centre 'Kurchatov Institute', Protvino, Russia
I. Azhgirey, I. Bayshev, S. Bitioukov, D. Elumakhov, A. Godizov, V. Kachanov, A. Kalinin, D. Konstantinov, P. Mandrik, V. Petrov, R. Ryutin, S. Slabospitskii, A. Sobol, S. Troshin, N. Tyurin, A. Uzunian, A. Volkov

National Research Tomsk Polytechnic University, Tomsk, Russia
A. Babaev, S. Baidali

University of Belgrade, Faculty of Physics and Vinca Institute of Nuclear Sciences, Belgrade, Serbia
P. Adzic[42], P. Cirkovic, D. Devetak, M. Dordevic, J. Milosevic

Centro de Investigaciones Energéticas Medioambientales y Tecnológicas (CIEMAT), Madrid, Spain
J. Alcaraz Maestre, A. Álvarez Fernández, I. Bachiller, M. Barrio Luna, J.A. Brochero Cifuentes, M. Cerrada, N. Colino, B. De La Cruz, A. Delgado Peris, C. Fernandez Bedoya, J.P. Fernández Ramos, J. Flix, M.C. Fouz, O. Gonzalez Lopez, S. Goy Lopez, J.M. Hernandez, M.I. Josa, D. Moran, A. Pérez-Calero Yzquierdo, J. Puerta Pelayo, I. Redondo, L. Romero, M.S. Soares, A. Triossi

Universidad Autónoma de Madrid, Madrid, Spain
C. Albajar, J.F. de Trocóniz

Universidad de Oviedo, Oviedo, Spain
J. Cuevas, C. Erice, J. Fernandez Menendez, S. Folgueras, I. Gonzalez Caballero, J.R. González Fernández, E. Palencia Cortezon, V. Rodríguez Bouza, S. Sanchez Cruz, P. Vischia, J.M. Vizan Garcia

Instituto de Física de Cantabria (IFCA), CSIC-Universidad de Cantabria, Santander, Spain
I.J. Cabrillo, A. Calderon, B. Chazin Quero, J. Duarte Campderros, M. Fernandez, P.J. Fernández Manteca, A. García Alonso, J. Garcia-Ferrero, G. Gomez, A. Lopez Virto, J. Marco, C. Martinez Rivero, P. Martinez Ruiz del Arbol, F. Matorras, J. Piedra Gomez, C. Prieels, T. Rodrigo, A. Ruiz-Jimeno, L. Scodellaro, N. Trevisani, I. Vila, R. Vilar Cortabitarte

CERN, European Organization for Nuclear Research, Geneva, Switzerland
D. Abbaneo, B. Akgun, E. Auffray, P. Baillon, A.H. Ball, D. Barney, J. Bendavid, M. Bianco, A. Bocci, C. Botta, T. Camporesi, M. Cepeda, G. Cerminara, E. Chapon, Y. Chen, G. Cucciati, D. d'Enterria, A. Dabrowski, V. Daponte, A. David, A. De Roeck, N. Deelen, M. Dobson, T. du Pree, M. Dünser, N. Dupont, A. Elliott-Peisert, P. Everaerts, F. Fallavollita[43], D. Fasanella,

G. Franzoni, J. Fulcher, W. Funk, D. Gigi, A. Gilbert, K. Gill, F. Glege, M. Guilbaud, D. Gulhan, J. Hegeman, V. Innocente, A. Jafari, P. Janot, O. Karacheban[18], J. Kieseler, A. Kornmayer, M. Krammer[1], C. Lange, P. Lecoq, C. Lourenço, L. Malgeri, M. Mannelli, F. Meijers, J.A. Merlin, S. Mersi, E. Meschi, P. Milenovic[44], F. Moortgat, M. Mulders, J. Ngadiuba, S. Orfanelli, L. Orsini, F. Pantaleo[15], L. Pape, E. Perez, M. Peruzzi, A. Petrilli, G. Petrucciani, A. Pfeiffer, M. Pierini, F.M. Pitters, D. Rabady, A. Racz, T. Reis, G. Rolandi[45], M. Rovere, H. Sakulin, C. Schäfer, C. Schwick, M. Seidel, M. Selvaggi, A. Sharma, P. Silva, P. Sphicas[46], A. Stakia, J. Steggemann, M. Tosi, D. Treille, A. Tsirou, V. Veckalns[47], W.D. Zeuner

Paul Scherrer Institut, Villigen, Switzerland
L. Caminada[48], K. Deiters, W. Erdmann, R. Horisberger, Q. Ingram, H.C. Kaestli, D. Kotlinski, U. Langenegger, T. Rohe, S.A. Wiederkehr

ETH Zurich - Institute for Particle Physics and Astrophysics (IPA), Zurich, Switzerland
M. Backhaus, L. Bäni, P. Berger, N. Chernyavskaya, G. Dissertori, M. Dittmar, M. Donegà, C. Dorfer, C. Grab, C. Heidegger, D. Hits, J. Hoss, T. Klijnsma, W. Lustermann, R.A. Manzoni, M. Marionneau, M.T. Meinhard, F. Micheli, P. Musella, F. Nessi-Tedaldi, J. Pata, F. Pauss, G. Perrin, L. Perrozzi, S. Pigazzini, M. Quittnat, D. Ruini, D.A. Sanz Becerra, M. Schönenberger, L. Shchutska, V.R. Tavolaro, K. Theofilatos, M.L. Vesterbacka Olsson, R. Wallny, D.H. Zhu

Universität Zürich, Zurich, Switzerland
T.K. Aarrestad, C. Amsler[49], D. Brzhechko, M.F. Canelli, A. De Cosa, R. Del Burgo, S. Donato, C. Galloni, T. Hreus, B. Kilminster, I. Neutelings, D. Pinna, G. Rauco, P. Robmann, D. Salerno, K. Schweiger, C. Seitz, Y. Takahashi, A. Zucchetta

National Central University, Chung-Li, Taiwan
Y.H. Chang, K.y. Cheng, T.H. Doan, Sh. Jain, R. Khurana, C.M. Kuo, W. Lin, A. Pozdnyakov, S.S. Yu

National Taiwan University (NTU), Taipei, Taiwan
P. Chang, Y. Chao, K.F. Chen, P.H. Chen, W.-S. Hou, Arun Kumar, Y.y. Li, R.-S. Lu, E. Paganis, A. Psallidas, A. Steen, J.f. Tsai

Chulalongkorn University, Faculty of Science, Department of Physics, Bangkok, Thailand
B. Asavapibhop, N. Srimanobhas, N. Suwonjandee

Çukurova University, Physics Department, Science and Art Faculty, Adana, Turkey
A. Bat, F. Boran, S. Damarseckin, Z.S. Demiroglu, F. Dolek, C. Dozen, I. Dumanoglu, S. Girgis, G. Gokbulut, Y. Guler, E. Gurpinar, I. Hos[50], C. Isik, E.E. Kangal[51], O. Kara, A. Kayis Topaksu, U. Kiminsu, M. Oglakci, G. Onengut, K. Ozdemir[52], S. Ozturk[53], D. Sunar Cerci[54], B. Tali[54], U.G. Tok, H. Topakli[53], S. Turkcapar, I.S. Zorbakir, C. Zorbilmez

Middle East Technical University, Physics Department, Ankara, Turkey
B. Isildak[55], G. Karapinar[56], M. Yalvac, M. Zeyrek

Bogazici University, Istanbul, Turkey
I.O. Atakisi, E. Gülmez, M. Kaya[57], O. Kaya[58], S. Ozkorucuklu[59], S. Tekten, E.A. Yetkin[60]

Istanbul Technical University, Istanbul, Turkey
M.N. Agaras, S. Atay, A. Cakir, K. Cankocak, Y. Komurcu, S. Sen[61]

Institute for Scintillation Materials of National Academy of Science of Ukraine, Kharkov, Ukraine
B. Grynyov

National Scientific Center, Kharkov Institute of Physics and Technology, Kharkov, Ukraine
L. Levchuk

University of Bristol, Bristol, United Kingdom
F. Ball, L. Beck, J.J. Brooke, D. Burns, E. Clement, D. Cussans, O. Davignon, H. Flacher, J. Goldstein, G.P. Heath, H.F. Heath, L. Kreczko, D.M. Newbold[62], S. Paramesvaran, B. Penning, T. Sakuma, D. Smith, V.J. Smith, J. Taylor, A. Titterton

Rutherford Appleton Laboratory, Didcot, United Kingdom
K.W. Bell, A. Belyaev[63], C. Brew, R.M. Brown, D. Cieri, D.J.A. Cockerill, J.A. Coughlan, K. Harder, S. Harper, J. Linacre, E. Olaiya, D. Petyt, C.H. Shepherd-Themistocleous, A. Thea, I.R. Tomalin, T. Williams, W.J. Womersley

Imperial College, London, United Kingdom
G. Auzinger, R. Bainbridge, P. Bloch, J. Borg, S. Breeze, O. Buchmuller, A. Bundock, S. Casasso, D. Colling, L. Corpe, P. Dauncey, G. Davies, M. Della Negra, R. Di Maria, Y. Haddad, G. Hall, G. Iles, T. James, M. Komm, C. Laner, L. Lyons, A.-M. Magnan, S. Malik, A. Martelli, J. Nash[64], A. Nikitenko[6], V. Palladino, M. Pesaresi, A. Richards, A. Rose, E. Scott, C. Seez, A. Shtipliyski, G. Singh, M. Stoye, T. Strebler, S. Summers, A. Tapper, K. Uchida, T. Virdee[15], N. Wardle, D. Winterbottom, J. Wright, S.C. Zenz

Brunel University, Uxbridge, United Kingdom
J.E. Cole, P.R. Hobson, A. Khan, P. Kyberd, C.K. Mackay, A. Morton, I.D. Reid, L. Teodorescu, S. Zahid

Baylor University, Waco, USA
K. Call, J. Dittmann, K. Hatakeyama, H. Liu, C. Madrid, B. Mcmaster, N. Pastika, C. Smith

Catholic University of America, Washington DC, USA
R. Bartek, A. Dominguez

The University of Alabama, Tuscaloosa, USA
A. Buccilli, S.I. Cooper, C. Henderson, P. Rumerio, C. West

Boston University, Boston, USA
D. Arcaro, T. Bose, D. Gastler, D. Rankin, C. Richardson, J. Rohlf, L. Sulak, D. Zou

Brown University, Providence, USA
G. Benelli, X. Coubez, D. Cutts, M. Hadley, J. Hakala, U. Heintz, J.M. Hogan[65], K.H.M. Kwok, E. Laird, G. Landsberg, J. Lee, Z. Mao, M. Narain, J. Pazzini, S. Piperov, S. Sagir[66], R. Syarif, E. Usai, D. Yu

University of California, Davis, Davis, USA
R. Band, C. Brainerd, R. Breedon, D. Burns, M. Calderon De La Barca Sanchez, M. Chertok, J. Conway, R. Conway, P.T. Cox, R. Erbacher, C. Flores, G. Funk, W. Ko, O. Kukral, R. Lander, C. Mclean, M. Mulhearn, D. Pellett, J. Pilot, S. Shalhout, M. Shi, D. Stolp, D. Taylor, K. Tos, M. Tripathi, Z. Wang, F. Zhang

University of California, Los Angeles, USA
M. Bachtis, C. Bravo, R. Cousins, A. Dasgupta, A. Florent, J. Hauser, M. Ignatenko, N. Mccoll, S. Regnard, D. Saltzberg, C. Schnaible, V. Valuev

University of California, Riverside, Riverside, USA
E. Bouvier, K. Burt, R. Clare, J.W. Gary, S.M.A. Ghiasi Shirazi, G. Hanson, G. Karapostoli,

E. Kennedy, F. Lacroix, O.R. Long, M. Olmedo Negrete, M.I. Paneva, W. Si, L. Wang, H. Wei, S. Wimpenny, B.R. Yates

University of California, San Diego, La Jolla, USA
J.G. Branson, S. Cittolin, M. Derdzinski, R. Gerosa, D. Gilbert, B. Hashemi, A. Holzner, D. Klein, G. Kole, V. Krutelyov, J. Letts, M. Masciovecchio, D. Olivito, S. Padhi, M. Pieri, M. Sani, V. Sharma, S. Simon, M. Tadel, A. Vartak, S. Wasserbaech[67], J. Wood, F. Würthwein, A. Yagil, G. Zevi Della Porta

University of California, Santa Barbara - Department of Physics, Santa Barbara, USA
N. Amin, R. Bhandari, J. Bradmiller-Feld, C. Campagnari, M. Citron, A. Dishaw, V. Dutta, M. Franco Sevilla, L. Gouskos, R. Heller, J. Incandela, A. Ovcharova, H. Qu, J. Richman, D. Stuart, I. Suarez, S. Wang, J. Yoo

California Institute of Technology, Pasadena, USA
D. Anderson, A. Bornheim, J.M. Lawhorn, H.B. Newman, T.Q. Nguyen, M. Spiropulu, J.R. Vlimant, R. Wilkinson, S. Xie, Z. Zhang, R.Y. Zhu

Carnegie Mellon University, Pittsburgh, USA
M.B. Andrews, T. Ferguson, T. Mudholkar, M. Paulini, M. Sun, I. Vorobiev, M. Weinberg

University of Colorado Boulder, Boulder, USA
J.P. Cumalat, W.T. Ford, F. Jensen, A. Johnson, M. Krohn, S. Leontsinis, E. MacDonald, T. Mulholland, K. Stenson, K.A. Ulmer, S.R. Wagner

Cornell University, Ithaca, USA
J. Alexander, J. Chaves, Y. Cheng, J. Chu, A. Datta, K. Mcdermott, N. Mirman, J.R. Patterson, D. Quach, A. Rinkevicius, A. Ryd, L. Skinnari, L. Soffi, S.M. Tan, Z. Tao, J. Thom, J. Tucker, P. Wittich, M. Zientek

Fermi National Accelerator Laboratory, Batavia, USA
S. Abdullin, M. Albrow, M. Alyari, G. Apollinari, A. Apresyan, A. Apyan, S. Banerjee, L.A.T. Bauerdick, A. Beretvas, J. Berryhill, P.C. Bhat, G. Bolla[†], K. Burkett, J.N. Butler, A. Canepa, G.B. Cerati, H.W.K. Cheung, F. Chlebana, M. Cremonesi, J. Duarte, V.D. Elvira, J. Freeman, Z. Gecse, E. Gottschalk, L. Gray, D. Green, S. Grünendahl, O. Gutsche, J. Hanlon, R.M. Harris, S. Hasegawa, J. Hirschauer, Z. Hu, B. Jayatilaka, S. Jindariani, M. Johnson, U. Joshi, B. Klima, M.J. Kortelainen, B. Kreis, S. Lammel, D. Lincoln, R. Lipton, M. Liu, T. Liu, J. Lykken, K. Maeshima, J.M. Marraffino, D. Mason, P. McBride, P. Merkel, S. Mrenna, S. Nahn, V. O'Dell, K. Pedro, C. Pena, O. Prokofyev, G. Rakness, L. Ristori, A. Savoy-Navarro[68], B. Schneider, E. Sexton-Kennedy, A. Soha, W.J. Spalding, L. Spiegel, S. Stoynev, J. Strait, N. Strobbe, L. Taylor, S. Tkaczyk, N.V. Tran, L. Uplegger, E.W. Vaandering, C. Vernieri, M. Verzocchi, R. Vidal, M. Wang, H.A. Weber, A. Whitbeck

University of Florida, Gainesville, USA
D. Acosta, P. Avery, P. Bortignon, D. Bourilkov, A. Brinkerhoff, L. Cadamuro, A. Carnes, M. Carver, D. Curry, R.D. Field, S.V. Gleyzer, B.M. Joshi, J. Konigsberg, A. Korytov, P. Ma, K. Matchev, H. Mei, G. Mitselmakher, K. Shi, D. Sperka, J. Wang, S. Wang

Florida International University, Miami, USA
Y.R. Joshi, S. Linn

Florida State University, Tallahassee, USA
A. Ackert, T. Adams, A. Askew, S. Hagopian, V. Hagopian, K.F. Johnson, T. Kolberg, G. Martinez, T. Perry, H. Prosper, A. Saha, A. Santra, V. Sharma, R. Yohay

Florida Institute of Technology, Melbourne, USA
M.M. Baarmand, V. Bhopatkar, S. Colafranceschi, M. Hohlmann, D. Noonan, M. Rahmani, T. Roy, F. Yumiceva

University of Illinois at Chicago (UIC), Chicago, USA
M.R. Adams, L. Apanasevich, D. Berry, R.R. Betts, R. Cavanaugh, X. Chen, S. Dittmer, O. Evdokimov, C.E. Gerber, D.A. Hangal, D.J. Hofman, K. Jung, J. Kamin, C. Mills, I.D. Sandoval Gonzalez, M.B. Tonjes, N. Varelas, H. Wang, X. Wang, Z. Wu, J. Zhang

The University of Iowa, Iowa City, USA
M. Alhusseini, B. Bilki[69], W. Clarida, K. Dilsiz[70], S. Durgut, R.P. Gandrajula, M. Haytmyradov, V. Khristenko, J.-P. Merlo, A. Mestvirishvili, A. Moeller, J. Nachtman, H. Ogul[71], Y. Onel, F. Ozok[72], A. Penzo, C. Snyder, E. Tiras, J. Wetzel

Johns Hopkins University, Baltimore, USA
B. Blumenfeld, A. Cocoros, N. Eminizer, D. Fehling, L. Feng, A.V. Gritsan, W.T. Hung, P. Maksimovic, J. Roskes, U. Sarica, M. Swartz, M. Xiao, C. You

The University of Kansas, Lawrence, USA
A. Al-bataineh, P. Baringer, A. Bean, S. Boren, J. Bowen, A. Bylinkin, J. Castle, S. Khalil, A. Kropivnitskaya, D. Majumder, W. Mcbrayer, M. Murray, C. Rogan, S. Sanders, E. Schmitz, J.D. Tapia Takaki, Q. Wang

Kansas State University, Manhattan, USA
A. Ivanov, K. Kaadze, D. Kim, Y. Maravin, D.R. Mendis, T. Mitchell, A. Modak, A. Mohammadi, L.K. Saini, N. Skhirtladze

Lawrence Livermore National Laboratory, Livermore, USA
F. Rebassoo, D. Wright

University of Maryland, College Park, USA
A. Baden, O. Baron, A. Belloni, S.C. Eno, Y. Feng, C. Ferraioli, N.J. Hadley, S. Jabeen, G.Y. Jeng, R.G. Kellogg, J. Kunkle, A.C. Mignerey, F. Ricci-Tam, Y.H. Shin, A. Skuja, S.C. Tonwar, K. Wong

Massachusetts Institute of Technology, Cambridge, USA
D. Abercrombie, B. Allen, V. Azzolini, A. Baty, G. Bauer, R. Bi, S. Brandt, W. Busza, I.A. Cali, M. D'Alfonso, Z. Demiragli, G. Gomez Ceballos, M. Goncharov, P. Harris, D. Hsu, M. Hu, Y. Iiyama, G.M. Innocenti, M. Klute, D. Kovalskyi, Y.-J. Lee, P.D. Luckey, B. Maier, A.C. Marini, C. Mcginn, C. Mironov, S. Narayanan, X. Niu, C. Paus, C. Roland, G. Roland, G.S.F. Stephans, K. Sumorok, K. Tatar, D. Velicanu, J. Wang, T.W. Wang, B. Wyslouch, S. Zhaozhong

University of Minnesota, Minneapolis, USA
A.C. Benvenuti, R.M. Chatterjee, A. Evans, P. Hansen, S. Kalafut, Y. Kubota, Z. Lesko, J. Mans, S. Nourbakhsh, N. Ruckstuhl, R. Rusack, J. Turkewitz, M.A. Wadud

University of Mississippi, Oxford, USA
J.G. Acosta, S. Oliveros

University of Nebraska-Lincoln, Lincoln, USA
E. Avdeeva, K. Bloom, D.R. Claes, C. Fangmeier, F. Golf, R. Gonzalez Suarez, R. Kamalieddin, I. Kravchenko, J. Monroy, J.E. Siado, G.R. Snow, B. Stieger

State University of New York at Buffalo, Buffalo, USA
A. Godshalk, C. Harrington, I. Iashvili, A. Kharchilava, D. Nguyen, A. Parker, S. Rappoccio, B. Roozbahani

Northeastern University, Boston, USA
G. Alverson, E. Barberis, C. Freer, A. Hortiangtham, D.M. Morse, T. Orimoto, R. Teixeira De Lima, T. Wamorkar, B. Wang, A. Wisecarver, D. Wood

Northwestern University, Evanston, USA
S. Bhattacharya, O. Charaf, K.A. Hahn, N. Mucia, N. Odell, M.H. Schmitt, K. Sung, M. Trovato, M. Velasco

University of Notre Dame, Notre Dame, USA
R. Bucci, N. Dev, M. Hildreth, K. Hurtado Anampa, C. Jessop, D.J. Karmgard, N. Kellams, K. Lannon, W. Li, N. Loukas, N. Marinelli, F. Meng, C. Mueller, Y. Musienko[34], M. Planer, A. Reinsvold, R. Ruchti, P. Siddireddy, G. Smith, S. Taroni, M. Wayne, A. Wightman, M. Wolf, A. Woodard

The Ohio State University, Columbus, USA
J. Alimena, L. Antonelli, B. Bylsma, L.S. Durkin, S. Flowers, B. Francis, A. Hart, C. Hill, W. Ji, T.Y. Ling, W. Luo, B.L. Winer, H.W. Wulsin

Princeton University, Princeton, USA
S. Cooperstein, P. Elmer, J. Hardenbrook, P. Hebda, S. Higginbotham, A. Kalogeropoulos, D. Lange, M.T. Lucchini, J. Luo, D. Marlow, K. Mei, I. Ojalvo, J. Olsen, C. Palmer, P. Piroué, J. Salfeld-Nebgen, D. Stickland, C. Tully

University of Puerto Rico, Mayaguez, USA
S. Malik, S. Norberg

Purdue University, West Lafayette, USA
A. Barker, V.E. Barnes, S. Das, L. Gutay, M. Jones, A.W. Jung, A. Khatiwada, B. Mahakud, D.H. Miller, N. Neumeister, C.C. Peng, H. Qiu, J.F. Schulte, J. Sun, F. Wang, R. Xiao, W. Xie

Purdue University Northwest, Hammond, USA
T. Cheng, J. Dolen, N. Parashar

Rice University, Houston, USA
Z. Chen, K.M. Ecklund, S. Freed, F.J.M. Geurts, M. Kilpatrick, W. Li, B. Michlin, B.P. Padley, J. Roberts, J. Rorie, W. Shi, Z. Tu, J. Zabel, A. Zhang

University of Rochester, Rochester, USA
A. Bodek, P. de Barbaro, R. Demina, Y.t. Duh, J.L. Dulemba, C. Fallon, T. Ferbel, M. Galanti, A. Garcia-Bellido, J. Han, O. Hindrichs, A. Khukhunaishvili, K.H. Lo, P. Tan, R. Taus, M. Verzetti

Rutgers, The State University of New Jersey, Piscataway, USA
A. Agapitos, J.P. Chou, Y. Gershtein, T.A. Gómez Espinosa, E. Halkiadakis, M. Heindl, E. Hughes, S. Kaplan, R. Kunnawalkam Elayavalli, S. Kyriacou, A. Lath, R. Montalvo, K. Nash, M. Osherson, H. Saka, S. Salur, S. Schnetzer, D. Sheffield, S. Somalwar, R. Stone, S. Thomas, P. Thomassen, M. Walker

University of Tennessee, Knoxville, USA
A.G. Delannoy, J. Heideman, G. Riley, K. Rose, S. Spanier, K. Thapa

Texas A&M University, College Station, USA
O. Bouhali[31], A. Celik, M. Dalchenko, M. De Mattia, A. Delgado, S. Dildick, R. Eusebi, J. Gilmore, T. Huang, T. Kamon[73], S. Luo, R. Mueller, Y. Pakhotin, R. Patel, A. Perloff, L. Perniè, D. Rathjens, A. Safonov, A. Tatarinov

Texas Tech University, Lubbock, USA
N. Akchurin, J. Damgov, F. De Guio, P.R. Dudero, S. Kunori, K. Lamichhane, S.W. Lee, T. Mengke, S. Muthumuni, T. Peltola, S. Undleeb, I. Volobouev, Z. Wang

Vanderbilt University, Nashville, USA
S. Greene, A. Gurrola, R. Janjam, W. Johns, C. Maguire, A. Melo, H. Ni, K. Padeken, J.D. Ruiz Alvarez, P. Sheldon, S. Tuo, J. Velkovska, M. Verweij, Q. Xu

University of Virginia, Charlottesville, USA
M.W. Arenton, P. Barria, B. Cox, R. Hirosky, M. Joyce, A. Ledovskoy, H. Li, C. Neu, T. Sinthuprasith, Y. Wang, E. Wolfe, F. Xia

Wayne State University, Detroit, USA
R. Harr, P.E. Karchin, N. Poudyal, J. Sturdy, P. Thapa, S. Zaleski

University of Wisconsin - Madison, Madison, WI, USA
M. Brodski, J. Buchanan, C. Caillol, D. Carlsmith, S. Dasu, L. Dodd, S. Duric, B. Gomber, M. Grothe, M. Herndon, A. Hervé, U. Hussain, P. Klabbers, A. Lanaro, A. Levine, K. Long, R. Loveless, T. Ruggles, A. Savin, N. Smith, W.H. Smith, N. Woods

†: Deceased
1: Also at Vienna University of Technology, Vienna, Austria
2: Also at IRFU, CEA, Université Paris-Saclay, Gif-sur-Yvette, France
3: Also at Universidade Estadual de Campinas, Campinas, Brazil
4: Also at Federal University of Rio Grande do Sul, Porto Alegre, Brazil
5: Also at Université Libre de Bruxelles, Bruxelles, Belgium
6: Also at Institute for Theoretical and Experimental Physics, Moscow, Russia
7: Also at Joint Institute for Nuclear Research, Dubna, Russia
8: Also at Cairo University, Cairo, Egypt
9: Also at Helwan University, Cairo, Egypt
10: Now at Zewail City of Science and Technology, Zewail, Egypt
11: Also at Department of Physics, King Abdulaziz University, Jeddah, Saudi Arabia
12: Also at Université de Haute Alsace, Mulhouse, France
13: Also at Skobeltsyn Institute of Nuclear Physics, Lomonosov Moscow State University, Moscow, Russia
14: Also at Tbilisi State University, Tbilisi, Georgia
15: Also at CERN, European Organization for Nuclear Research, Geneva, Switzerland
16: Also at RWTH Aachen University, III. Physikalisches Institut A, Aachen, Germany
17: Also at University of Hamburg, Hamburg, Germany
18: Also at Brandenburg University of Technology, Cottbus, Germany
19: Also at MTA-ELTE Lendület CMS Particle and Nuclear Physics Group, Eötvös Loránd University, Budapest, Hungary
20: Also at Institute of Nuclear Research ATOMKI, Debrecen, Hungary
21: Also at Institute of Physics, University of Debrecen, Debrecen, Hungary
22: Also at Indian Institute of Technology Bhubaneswar, Bhubaneswar, India
23: Also at Institute of Physics, Bhubaneswar, India
24: Also at Shoolini University, Solan, India
25: Also at University of Visva-Bharati, Santiniketan, India
26: Also at Isfahan University of Technology, Isfahan, Iran
27: Also at Plasma Physics Research Center, Science and Research Branch, Islamic Azad University, Tehran, Iran
28: Also at Università degli Studi di Siena, Siena, Italy

29: Also at International Islamic University of Malaysia, Kuala Lumpur, Malaysia

30: Also at Malaysian Nuclear Agency, MOSTI, Kajang, Malaysia

31: Also at Texas A&M University at Qatar, Doha, Qatar

32: Also at Consejo Nacional de Ciencia y Tecnología, Mexico city, Mexico

33: Also at Warsaw University of Technology, Institute of Electronic Systems, Warsaw, Poland

34: Also at Institute for Nuclear Research, Moscow, Russia

35: Now at National Research Nuclear University 'Moscow Engineering Physics Institute' (MEPhI), Moscow, Russia

36: Also at Institute of Nuclear Physics of the Uzbekistan Academy of Sciences, Tashkent, Uzbekistan

37: Also at St. Petersburg State Polytechnical University, St. Petersburg, Russia

38: Also at University of Florida, Gainesville, USA

39: Also at P.N. Lebedev Physical Institute, Moscow, Russia

40: Also at California Institute of Technology, Pasadena, USA

41: Also at Budker Institute of Nuclear Physics, Novosibirsk, Russia

42: Also at Faculty of Physics, University of Belgrade, Belgrade, Serbia

43: Also at INFN Sezione di Pavia [a], Università di Pavia [b], Pavia, Italy

44: Also at University of Belgrade, Faculty of Physics and Vinca Institute of Nuclear Sciences, Belgrade, Serbia

45: Also at Scuola Normale e Sezione dell'INFN, Pisa, Italy

46: Also at National and Kapodistrian University of Athens, Athens, Greece

47: Also at Riga Technical University, Riga, Latvia

48: Also at Universität Zürich, Zurich, Switzerland

49: Also at Stefan Meyer Institute for Subatomic Physics (SMI), Vienna, Austria

50: Also at Istanbul Aydin University, Istanbul, Turkey

51: Also at Mersin University, Mersin, Turkey

52: Also at Piri Reis University, Istanbul, Turkey

53: Also at Gaziosmanpasa University, Tokat, Turkey

54: Also at Adiyaman University, Adiyaman, Turkey

55: Also at Ozyegin University, Istanbul, Turkey

56: Also at Izmir Institute of Technology, Izmir, Turkey

57: Also at Marmara University, Istanbul, Turkey

58: Also at Kafkas University, Kars, Turkey

59: Also at Istanbul University, Faculty of Science, Istanbul, Turkey

60: Also at Istanbul Bilgi University, Istanbul, Turkey

61: Also at Hacettepe University, Ankara, Turkey

62: Also at Rutherford Appleton Laboratory, Didcot, United Kingdom

63: Also at School of Physics and Astronomy, University of Southampton, Southampton, United Kingdom

64: Also at Monash University, Faculty of Science, Clayton, Australia

65: Also at Bethel University, St. Paul, USA

66: Also at Karamanoğlu Mehmetbey University, Karaman, Turkey

67: Also at Utah Valley University, Orem, USA

68: Also at Purdue University, West Lafayette, USA

69: Also at Beykent University, Istanbul, Turkey

70: Also at Bingol University, Bingol, Turkey

71: Also at Sinop University, Sinop, Turkey

72: Also at Mimar Sinan University, Istanbul, Istanbul, Turkey

73: Also at Kyungpook National University, Daegu, Korea